A Stochastic Framework for Real-Time Quantum Field Dynamics

Xiao Lin*
Beijing, China

2026-03-29

Abstract

We propose a Stochastic Formulation that establishes a direct mathematical correspondence between the real-time Feynman path integral in Minkowski spacetime and the expectation values of classical stochastic processes. This framework offers an alternative approach to quantum dynamics by formulating evolution through intrinsic stochastic processes rather than relying solely on pre-discretized spacetime backgrounds. Specifically, we demonstrate that the unitary dynamics of scalar fields can be mapped to continuous Wiener processes, while spinor fields correspond to discrete Poisson jump processes. Distinct from conventional methods involving perturbative expansions, Euclideanization, or Grassmann algebra, our formulation provides a non-perturbative, real-time framework where quantum amplitudes are derived statistically from stochastic trajectories.

We implement this framework via a grid-based tree recursion scheme for the Klein-Gordon field, benchmarked against exact solutions of the forced harmonic oscillator. For the Dirac field, we derive an analytical closed-form finite difference scheme that effectively models its evolution. By integrating these schemes, we successfully apply the framework to the Yukawa coupling model and extend it to QED. Our results reveal non-trivial dynamical features, such as feedback-driven mass oscillations, offering complementary insights to standard perturbative descriptions. Crucially, the structural nature of this stochastic approach inherently avoids the fermion doubling and sign problems often encountered in lattice approach. These applications suggest a robust pathway for tackling complex systems, including gauge theories like QCD.

Key words: Quantum Field Theory, Feynman Path Integral, Stochastic Analysis, Wiener Process, Poisson Process.

*Email: xiao_lin_99@yahoo.com

1 Introduction

The Feynman path integral has provided quantum field theory (QFT) with a profound functional formulation based on the principle of least action. While conceptually elegant, its direct implementation in real-time Minkowski spacetime presents significant technical challenges due to the oscillatory nature of the integrand. To address these challenges, the community has developed powerful established frameworks, primarily perturbative expansions and lattice discretizations.

Perturbative methods, employing Feynman diagram techniques, have achieved remarkable success in weakly coupled regimes [1]. They serve as the cornerstone for precision calculations in the Standard Model. However, to fully explore the non-perturbative regime—essential for understanding phenomena such as dynamical mass generation and confinement—methods beyond the perturbation series are required.

Lattice field theory offers a robust non-perturbative alternative by discretizing spacetime, often utilizing a Euclidean formulation to map the path integral to a statistical partition function [2]. This approach has been highly successful in determining static properties and the spectrum of Quantum Chromodynamics (QCD). Nevertheless, the investigation of real-time dynamics and systems at finite density remains a frontier where standard Euclidean lattice techniques face inherent limitations. Specifically, the analytic continuation from Euclidean time is ill-posed for non-equilibrium processes, and the simulation of fermions in these regimes is computationally demanding due to the complex phase of the determinant. Consequently, there is a strong motivation to develop complementary approaches that operate directly within the Minkowski framework to investigate these deeper dynamical questions.

Other analytic approaches, such as instanton configurations or Schwinger-Dyson equations, provide valuable insights but often rely on specific approximations or truncations. Therefore, a direct numerical or analytic framework capable of handling time-dependent, strongly coupled systems in real time would provide a valuable addition to the existing theoretical toolkit.

We propose that these challenges can be addressed by revisiting the mathematical foundation of the path integral, specifically by relaxing the requirement for a rigid, pre-discretized

spacetime background. In this work, we introduce a stochastic framework that decouples quantum evolution from fixed spatial coordinates. Instead of treating space and time as a fundamental stage, we formulate dynamics as an *intrinsic stochastic process*, where physical observables emerge statistically from random trajectories. Specifically, we map scalar fields to continuous Wiener processes and spinor fields to discrete Poisson jump processes. This stochastic formulation operates without explicit spatial discretization or Grassmann variables. In this picture, particle "position" is derived as a statistical outcome of the stochastic flow rather than a primary grid variable. By establishing a structural isomorphism between the Minkowski path integral and classical stochastic expectations, we provide a direct, real-time framework for studying strongly coupled systems, naturally circumventing the constraints associated with Euclideanization and lattice artifacts.

The structure of this paper is as follows: Sections 2 and 3 detail the Wiener process formulation for the Klein-Gordon field, establishing a recursion scheme and validating its accuracy against exact solutions of the forced harmonic oscillator. Sections 4 and 5 construct the Poisson jump process formulation for the free Dirac spinor field, providing a stochastic bosonization of fermionic dynamics that inherently avoids the use of Grassmann algebra. Section 6 applies the full framework to the Yukawa coupling model, calculating the time-dependent evolution of the fermion effective mass and comparing the results with one-loop perturbation theory to illustrate non-perturbative dynamical effects. Finally, Section 7 extends this approach to Quantum Electrodynamics (QED), illustrating the framework's capability to handle gauge interactions and real-time photon-fermion dynamics, offering an alternative perspective to standard lattice formulations. Relevant analytic derivations are provided in the Appendices.

2 Stochastic formulation of the scalar field

Let $\phi(x)$ be a real massive Klein–Gordon scalar field, where $x = (t, \vec{x})$ denotes spacetime coordinates. Consider the coupling of the scalar field $\phi(x)$ to an external source $J(x)$. The Lagrangian density of the system is

$$\mathcal{L}(\phi, \partial_\mu \phi, J) = \frac{1}{2}(\partial_t \phi)^2 - \frac{1}{2}(\nabla \phi)^2 - \frac{1}{2}m^2\phi^2 + J(x)\phi(x). \tag{2.1}$$

According to quantum field theory, the transition amplitude from an initial state $|\phi_0, t_0\rangle$ to a final state $|\phi_T, T\rangle$ can be expressed as the following Feynman path integral:

$$\langle \phi_T, T \,|\, \phi_0, t_0 \rangle = \int \mathcal{D}\phi \, \exp\big[\mathrm{i}S\big] =: K(\phi_T, T; \phi_0, t_0), \tag{2.2}$$

where the action S is given by

$$S = \int \mathrm{d}^4x \, \mathcal{L}(\phi, \partial_\mu \phi, J). \tag{2.3}$$

Here $\phi_0 = \phi(t_0, \vec{x}_0)$, $\phi_T = \phi(T, \vec{x})$, and the integration measure $\mathrm{d}^4x = \mathrm{d}t\, \mathrm{d}^3x$ integrates t from t_0 to T and $\vec{x}$ over all space.

The physical interpretation of Eq. (2.2) is that the amplitude for the field variable ϕ to propagate from $(t_0, \vec{x}_0)$ to $(t, \vec{x})$ equals a weighted superposition of all possible field configurations $\mathcal{D}\phi$ between these two points, with the weight determined by the phase factor $\exp(\mathrm{i}S)$. This interpretation suggests that when the external source J is too complicated to allow an analytic solution for $\phi(x)$, one may attempt to obtain the transition amplitude by numerically simulating the possible paths of the field $\phi(x)$.

This paper focuses on the scenario where the field undergoes a localized excitation in space within a very short time interval, such as during an instantaneous high-energy collision in a particle accelerator. The long-term and large-scale evolution of the quantum field can be regarded as a superposition of numerous such localized excitations. To handle this situation, we attempt to introduce new degrees of freedom into the state function $\phi(t, \vec{x})$ to replace its dependence on the spatial coordinate $\vec{x}$. We therefore assume that the spatial variation of ϕ is concentrated near the origin, expressing $\phi(x)$ as a product of a function of t and a spherically symmetric exponential function of $\vec{x}$:

$$\phi(t, \vec{x}) = q(t)\, f_\kappa(\vec{x}) = q(t) e^{-\kappa r}. \tag{2.4}$$

Thus,

$$(\partial_t \phi)^2 = \dot{q}^2 e^{-2\kappa r}, \qquad (\nabla \phi)^2 = \kappa^2 q^2 e^{-2\kappa r}.$$

Substituting these into Eq. (2.3) and performing the spatial integration in spherical coordi-

nates yields:

$$\begin{aligned}\int \mathrm{d}^3x\, e^{-2\kappa r} &= 4\pi \int_0^\infty r^2 e^{-2\kappa r}\mathrm{d}r = \frac{4\pi}{(2\kappa)^3} = \frac{\pi}{2\kappa^3} \equiv I_0,\\ \int \mathrm{d}^3x\, (\nabla\phi)^2 &= \kappa^2 q^2 I_0.\end{aligned}$$

The total action then becomes:

$$S = \int \mathrm{d}^4x\, \mathcal{L} = \int_{t_0}^{T} \mathrm{d}t \Big[\frac{1}{2} I_0 \dot{q}^2 - \frac{1}{2}(\kappa^2 + m^2) I_0 q^2 + J\sqrt{I_0} q\Big]. \tag{2.5}$$

The constant factor in the Jq term has been absorbed into the source J for notational simplicity. The constant κ, which arises from the relativistic energy-momentum relation, represents the increase in effective mass due to high-energy states and can be determined experimentally based on collision velocities. Defining $\varphi(t) = \sqrt{I_0} q(t)$ and $\omega = \sqrt{\kappa^2 + m^2}$, the action simplifies to:

$$S = \int_{t_0}^{T} \mathrm{d}t \left[\frac{1}{2}\dot{\varphi}^2(t) - \frac{1}{2}\omega^2 \varphi^2(t) + J\varphi\right]. \tag{2.6}$$

Thus, we obtain the Feynman path integral formula for the transition amplitude of a free scalar field under a localized excitation driven by an external source J:

$$K = \int \mathcal{D}\varphi \exp\left\{\mathrm{i}\int_{t_0}^{T} \mathrm{d}t \left[\frac{1}{2}\dot{\varphi}^2(t) - \frac{1}{2}\omega^2\varphi^2(t) + J\varphi\right]\right\}. \tag{2.7}$$

To obtain the path distribution for the evolution of φ, we follow Feynman's approach [5] by discretizing the time interval $[t_0, T]$ into N equal segments of length $\Delta t = (T - t_0)/N$. Denote the n-th time point as $t^n = t_0 + n\Delta t$, and let φ^n represent the value of $\varphi(t)$ in the interval $[t^n, t^{n+1})$. The action S can then be expressed as:

$$S = \sum_{n=0}^{N-1} \Delta t \Big[\frac{1}{2}\Big(\frac{\varphi^{n+1} - \varphi^n}{\Delta t}\Big)^2 - \frac{1}{2}\omega^2 (\varphi^n)^2 + J\varphi^n\Big], \tag{2.8}$$

and the integration measure becomes:

$$\mathcal{D}\varphi = \frac{1}{\sqrt{2\pi\Delta t\,\mathrm{i}}} \prod_{n=1}^{N-1} \left[\int_{-\infty}^{\infty} \frac{\mathrm{d}\varphi^n}{\sqrt{2\pi\Delta t\,\mathrm{i}}}\right]. \tag{2.9}$$

The number of $\mathrm{d}\varphi^n$ is one less than the number of intervals N, because the initial point φ^0 and final point φ^N are fixed; the path integral is only defined over the $N-1$ intermediate time

points $t^1, t^2, \ldots, t^{N-1}$. However, for notational uniformity and analytical convenience, we treat the endpoint φ^N as a variable by adding an extra integration measure $\mathrm{d}\varphi^N/\sqrt{2\pi\Delta t\,\mathrm{i}}$. In numerical computations, specific values at desired points can be extracted accordingly. The initial point φ^0 is formally assigned a measure $\mathrm{d}\varphi^0 = \delta(\varphi^0 - \varphi(t_0))$, and the prefactor in $\mathcal{D}\varphi$ is absorbed into the product; special handling is applied during numerical implementation. Consequently, the transition amplitude can be written as:

$$\begin{aligned} K &= \prod_{n=0}^{N}\left[\int_{-\infty}^{\infty}\frac{\mathrm{d}\varphi^n}{\sqrt{2\pi\Delta t\,\mathrm{i}}}\right]\cdot\prod_{n=0}^{N}\left[\exp\left(\mathrm{i}\frac{(\varphi^{n+1}-\varphi^n)^2}{2\Delta t}-\frac{\mathrm{i}\Delta t}{2}\omega^2(\varphi^n)^2+\mathrm{i}\Delta t J\varphi^n\right)\right] \\ &= \prod_{n=0}^{N}\left\{\int_{-\infty}^{\infty}\frac{\mathrm{d}\varphi^n}{\sqrt{2\pi\Delta t\,\mathrm{i}}}\exp\left(\mathrm{i}\frac{(\varphi^{n+1}-\varphi^n)^2}{2\Delta t}-\frac{\mathrm{i}\Delta t}{2}\omega^2(\varphi^n)^2+\mathrm{i}\Delta t J\varphi^n\right)\right\}. \end{aligned} \tag{2.10}$$

Here φ^{N+1} can be regarded as the value of φ as $t\to\infty$, which does not affect our analysis.

We perform a change of integration variables by replacing all φ^n with $\sqrt{\mathrm{i}}\,u^n$, which leaves K unchanged. This yields:

$$\begin{aligned} K &= \prod_{n=0}^{N}\left\{\int_{-\infty}^{\infty}\frac{\mathrm{d}u^n}{\sqrt{2\pi\Delta t}}\exp\left(-\frac{(u^{n+1}-u^n)^2}{2\Delta t}+\frac{1}{2}\omega^2(u^n)^2\,\Delta t+\mathrm{i}^{3/2}Ju^n\,\Delta t\right)\right\} \\ &= \prod_{n=0}^{N}\left\{\int_{-\infty}^{\infty}\frac{\mathrm{d}u^n}{\sqrt{2\pi\Delta t}}\exp\left[-\frac{(u^{n+1}-u^n)^2}{2\Delta t}\right]\cdot\exp\left(\frac{1}{2}\omega^2(u^n)^2\,\Delta t+\mathrm{i}^{3/2}Ju^n\,\Delta t\right)\right\} \end{aligned} \tag{2.11}$$

It can be seen that each factor inside the product corresponds to a Gaussian measure. In probabilistic terms, each field variable u^n is a normally distributed random variable with mean equal to the next variable u^{n+1} and standard deviation $\sqrt{\Delta t}$. The probabilistic interpretation of the above expression is to take a mathematical expectation over the potential and coupling terms. Since the integration over u^n involves both $(u^{n+1}-u^n)^2$ and $(u^n-u^{n-1})^2$, the expectation is conditional. Hence, (2.11) can be written in the form of a conditional expectation:

$$K=\prod_{n=0}^{N}\left\{\mathbb{E}\left[\exp\left(\frac{1}{2}\omega^2(u^n)^2\,\Delta t+\mathrm{i}^{3/2}Ju^n\Delta t\right)\middle|u^{n-1},u^{n+1}\right]\right\}. \tag{2.12}$$

Alternatively, it can be expressed as a recursive chain:

$$K^{n+1}=\mathbb{E}\left[K^n\,\exp\left(\frac{1}{2}\omega^2(u^n)^2\,\Delta t+\mathrm{i}^{3/2}Ju^n\Delta t\right)\middle|u^{n+1}\right],\quad (n=0,\cdots,N). \tag{2.13}$$

This constitutes the stochastic formulation of the path integral.

Since the variables u^n are defined on distinct time intervals, they are mutually independent, and the sequence $\{u^n\}$ forms a Markov chain. In the limit $N \to \infty$ and $\Delta t \to 0$, $\{u^n\}$ converges to a continuous Wiener process (Brownian motion), defined by the following stochastic differential equation:

$$\mathrm{d}u = \sigma \, \mathrm{d}w(t), \tag{2.14}$$

where $w = w(t)$ is a Brownian motion and $\sigma > 0$ is a constant introduced for later convenience (for (2.11), $\sigma = 1$). In fact, this expression suggests that the evolution and coupling of bosons can be described by more elaborate models. In general, u can be represented as an Ornstein–Uhlenbeck process driven by multiple Brownian motions:

$$\mathrm{d}u = -\lambda u \, \mathrm{d}t + \sum_k \sigma_k \, \mathrm{d}w_k(t), \tag{2.15}$$

thereby introducing additional degrees of freedom and parameters to describe more complex particle evolution. This effectively augments the field φ with extra degrees of freedom: $\varphi = \varphi(t, w_1, w_2, \dots)$, compensating for the simplification of spatial dependence introduced by the localized excitation assumption.

Using the tower property of conditional expectations, the factors in (2.12) can be combined, and the final amplitude can be expressed as:

$$K = \mathbb{E}\left[\exp\left\{ \int_{t_0}^{T} \left(\frac{1}{2}\omega^2 u(t,w)^2 + \mathrm{i}^{3/2} J u(t,w) \right) \mathrm{d}t \right\} \right], \tag{2.16}$$

where the expectation $\mathbb{E}$ is taken over all Wiener process (Brownian motion) sample paths $u(t, w)$ defined by (2.14).

This equation indicates that for solving "point-to-point" transition amplitudes from an initial state $|\phi_0, t_0\rangle$ to a final state $|\phi_T, T\rangle$, it is not necessary to compute an expectation at each time step t^n. Instead, we integrate the function to be averaged along the sample paths prescribed by the Wiener process, evaluate the function at each Gaussian-distributed point at the final time T, and then take a single expectation. In other words, we can integrate along Wiener paths to obtain the distribution $K^T(\varphi)$ of K at time T, which corresponds to

a "point-to-surface" transition amplitude. We define this evolution operation as $\mathbb{K}$:

$$K^T(\varphi) = \mathbb{K}^u\left[\exp\left\{\int_{t_0}^{T}\left(\frac{1}{2}\omega^2 u(t,w)^2 + \mathrm{i}^{3/2}Ju(t,w)\right)\mathrm{d}t\right\}\right]. \tag{2.17}$$

Referring to (2.13), we can iteratively compute $K^n(u)$ by a conditional evolution at each time t^n as

$$K^{n+1}(\varphi) = \mathbb{K}^u\left[\exp\left(\frac{1}{2}\omega^2 u(t,w)^2\Delta t + \mathrm{i}^{3/2}Ju(t,w)\Delta t\right)\Big|\, t^n\right]K^n(\varphi), \quad (n=0,1,\cdots), \tag{2.18}$$

where the scalar $K^n(\varphi)$ is written on the right so that the same notation can be naturally extended to the matrix case. This stochastic formulation of the Feynman path integral provides a rigorous theoretical foundation for performing large-scale numerical simulations.

To the end of this section, we have three remarks:

First, the substitution $\varphi = \sqrt{\mathrm{i}}\, u$ should not be confused with the Wick rotation. While Wick rotation maps the path integral to the Feynman-Kac formula [6] by transforming real time to imaginary time, our approach strictly maintains physical time. It can be seen from (2.16) that, although our potential term $\frac{1}{2}\omega^2 u^2$ also becomes positive-definite, distinct from the Feynman-Kac formulation, it appears with a sign opposite to that of the kinetic term. This ensures that the total action does not become real and positive-definite, indicating that we are still describing quantum coherent evolution rather than thermal equilibrium.

Second, as seen from (2.17), the transition amplitude K is a function of time T and the bosonic field configuration φ. Since φ is driven by Brownian motion, the dependence of $K^T(\varphi)$ on φ exhibits a Gaussian-like distribution profile, which greatly facilitates the numerical evolution of K. However, it is crucial to emphasize that this distribution arises from the auxiliary stochastic process and is fundamentally distinct from the probability density defined in the quantum mechanical Hilbert space: $|K^T(\varphi)|^2$ is not the quantum mechanical probability density. The physical probability (or total transition amplitude) defined in quantum mechanics is independent of specific stochastic trajectories of φ. Its correct evaluation requires taking the expectation value of $K^T(\varphi)$ with respect to the Brownian motion measure (i.e., integrating over all φ), as given by:

$$\|K^T\| = \Big|\int_{-\infty}^{\infty} K^T(\varphi)\mathrm{d}\varphi\Big|. \tag{2.19}$$

Third, historically, Ord [7] and Jacobson & Schulman [8] also proposed a stochastic approach. In their work, stochastic terms are artificially added to the Euler–Lagrange equations of motion, leading to an Ornstein–Uhlenbeck process with drift terms given by the potential and the external source. It can be seen that their model equations not only deviate from Feynman's original conception of the path integral, but also alter the physical meaning of the parameters (such as ω) in the system under study. Therefore, their approach is distinct from the one presented here.

3 Numerical scheme for the scalar field

Numerical methods for stochastic processes generally fall into two categories: grid-based methods and Monte Carlo methods. In this section, we propose a grid-based approach to solve the scalar-field path integral problem formulated in terms of stochastic processes. Briefly stated, the continuous field variable $u(t, w)$ is discretized into a set of grid points $\{u_i^n\}$ at different times t^n and states w_i over the evolution period. Using the evolution law given by (2.14), we construct the transition probabilities for u moving between discrete points, as well as the survival probabilities upon reaching grid points. The transition amplitude and other results are then obtained by integrating along the paths in this probabilistic field according to (2.18). This grid-based method is analogous to the finite-difference schemes used in computational fluid dynamics.

The implementation of the grid method proceeds through the following steps:

Step 1. Discretize the evolution interval $[t_0, T]$ into small subintervals of length Δt. For simplicity, we assume uniform Δt; non-uniform partitions can be treated similarly. Denote the n-th time point as $t^n = t_0 + n\Delta t$.

Step 2. Construct the state grid for u. According to (2.14), the range of u expands with increasing time t under the influence of Brownian motion. Hence, the total width of the grid for u at time t should be proportional to the standard deviation $\sqrt{\mathbb{V}[u(t)]} = \sigma\sqrt{t}$. At each time layer t^n, we center the grid at $u = 0$ and take a total width of $20\sqrt{\mathbb{V}[u]}$ (i.e., extending $10\sqrt{\mathbb{V}[u]}$ on each side). This interval is then divided uniformly into $2I$ segments, yielding $2I+1$ equally spaced spatial grid points (we have chosen $I = 500$ in the following calculation

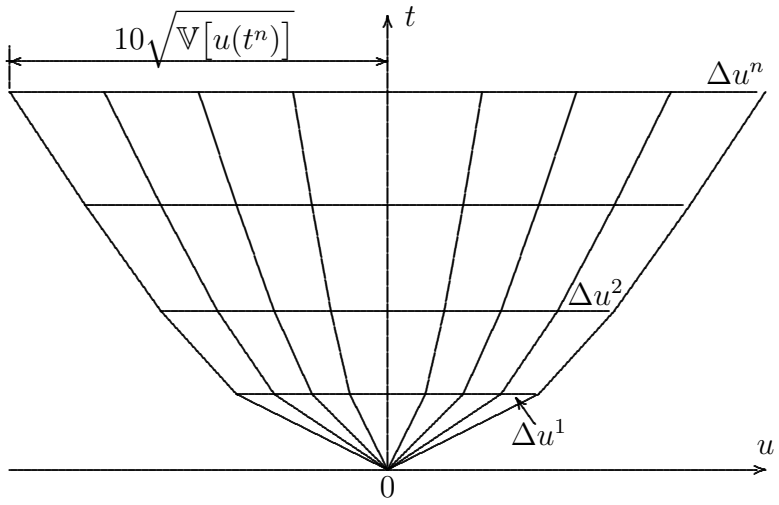

Figure 1: Diagram of a tree-structured grid.

example):

$$u_i^n = i\,\Delta u^n = i\left(\frac{10\sigma\sqrt{t^n}}{I}\right), \qquad (i = 0, \pm 1, \pm 2, \ldots, \pm I). \tag{3.1}$$

This results in a tree-like u-grid, as illustrated in Figure 1.

We emphasize that selecting the number of grid points I and the grid spacing Δu^n is critical for successful calculations. In our study, we dynamically monitor these parameters during computation for each specific problem, ensuring that the number of grid points is large enough to avoid boundary effects, and the grid spacing is fine enough to accurately resolve the simulated function distribution.

Step 3. Once the grid points are defined, we use the model equation to construct the transition probabilities for the amplitude. A multi-branch tree is employed to simulate the Brownian increment $\mathrm{d}w$. For an m-branch tree, the possible increments of $\mathrm{d}w$ over a time step Δt and their corresponding transition probabilities can be written as

$$\Delta w_k = \frac{2k - m - 1}{\sqrt{m-1}}\sqrt{\Delta t}, \qquad p_k = \frac{1}{2^{m-1}}\frac{(m-1)!}{(k-1)!\,(m-k)!}, \qquad (k = 1, 2, \ldots, m). \tag{3.2}$$

Here, we illustrate the method using a four-branch tree as an example. According to the model equation (2.14) together with (3.2), the state u_i^n can reach four intermediate points

at time t^{n+1} after a step Δt:

$$\begin{aligned} u_{\pm 1} &= u_i^n \pm \frac{1}{\sqrt{3}}\,\sigma\sqrt{\Delta t}, \\ u_{\pm 2} &= u_i^n \pm \sqrt{3}\,\sigma\sqrt{\Delta t}, \end{aligned} \tag{3.3}$$

where the transition probabilities of reaching u_{+1} or u_{-1} are 3/8, and those of reaching u_{+2} or u_{-2} are 1/8, as shown in Figure 2.

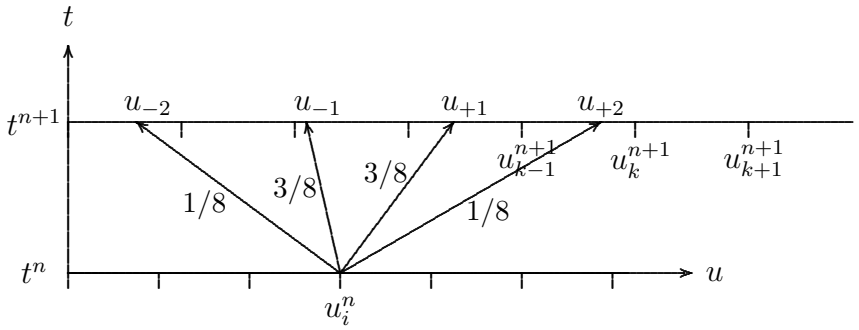

Figure 2: Transition probability between grid points.

In general, the intermediate points do not coincide exactly with the grid points at time t^{n+1}. For each intermediate point, we locate its three nearest neighboring grid points and redistribute the transition probability to these three grid points, thereby obtaining the grid-to-grid transition probabilities. For example, consider the intermediate point u_{+2}. Let u_k^{n+1} be the closest grid point and define

$$\eta = \frac{u_{+2} - u_k^{n+1}}{\Delta u^{n+1}}. \tag{3.4}$$

Using a second-order Taylor expansion, the value of a function $f(t^{n+1}, u)$ at $u = u_{+2}$ can be expressed as

$$\begin{aligned} f_{+2} &= f_k^{n+1} + \frac{\eta}{2}\big(f_{k+1}^{n+1} - f_{k-1}^{n+1}\big) + \frac{\eta^2}{2}\big(f_{k+1}^{n+1} - 2f_k^{n+1} + f_{k-1}^{n+1}\big) \\ &= \frac{1}{2}\big(\eta^2 - \eta\big) f_{k-1}^{n+1} + \big(1 - \eta^2\big) f_k^{n+1} + \frac{1}{2}\big(\eta^2 + \eta\big) f_{k+1}^{n+1}. \end{aligned} \tag{3.5}$$

Guided by this Taylor expansion, we assign the following transition probabilities from the intermediate point u_{+2} to the three neighboring grid points u_{k-1}^{n+1}, u_k^{n+1}, u_{k+1}^{n+1}:

$$\frac{1}{2}\big(\eta^2 - \eta\big), \qquad \big(1 - \eta^2\big), \qquad \frac{1}{2}\big(\eta^2 + \eta\big). \tag{3.6}$$

Multiplying each of these by 1/8 gives the transition probabilities from the starting grid point u_i^n via u_{+2} to the three target grid points. Repeating this procedure for the other three intermediate points u_{+1}, u_{-1}, u_{-2} and summing the contributions yields the complete set of transition probabilities from u_i^n to all grid points at time t^{n+1}.

We now provide a proof of the convergence and stability of the above algorithm. According to the requirements of stochastic analysis, this requires demonstrating that, within a time step Δt, the multi-branch tree scheme described above yields the same mathematical expectation and variance as the model equation (2.14). In the case of the four-branch tree described above, the mathematical expectation is

$$\mathbb{E}\Big[u_k^{n+1}\,\Big|\,u_i^n\Big] = \frac{3}{8}u_{+1} + \frac{3}{8}u_{-1} + \frac{1}{8}u_{+2} + \frac{1}{8}u_{-2} = u_i^n. \tag{3.7}$$

and the variance is

$$\begin{aligned}\mathbb{V}\Big[u_k^{n+1}\,\Big|\,u_i^n\Big] \;&=\; \frac{3}{8}(u_{+1}-u_i^n)^2 + \frac{3}{8}(u_{-1}-u_i^n)^2 \\ &\quad + \frac{1}{8}(u_{+2}-u_i^n)^2 + \frac{1}{8}(u_{-2}-u_i^n)^2 \;=\; \sigma^2\Delta t.\end{aligned} \tag{3.8}$$

Therefore, the expectation and variance values given by the four-branch tree scheme are in complete agreement with the model equation. Clearly, the multi-branch tree implemented using (3.2) can also yield the same results. Thus, the above multi-branch tree scheme is convergent and stable.

Step 4. Compute the evolution of the system's transition amplitude. According to (2.18), the transition amplitude is obtained by integrating along the paths of u. Therefore, while calculating the grid-to-grid transition probabilities for u, we also compute the amplitude at each grid point along the transferred paths.

Let K_i^n denote the amplitude at grid point i at time level n, and let p_{ik}^n be the transition probability from grid point u_i^n to u_k^{n+1}. The contribution to the amplitude at grid point k at time t^{n+1} from this particular path is

$$(K_k^{n+1})_i = K_i^n \,\exp\Big(\frac{1}{2}\omega^2(u_i^n)^2\Delta t + \mathrm{i}^{3/2}J(t^n)u_i^n\Delta t\Big)\,p_{ik}^n. \tag{3.9}$$

Summing over all starting grid points i at time level n gives the total amplitude arriving at

u_k^{n+1}:

$$K_k^{n+1} = \sum_{i=-I}^{I} K_i^n \, \exp\Big(\frac{1}{2}\omega^2 (u_i^n)^2 \Delta t + \mathrm{i}^{3/2} J(t^n) u_i^n \Delta t\Big)\, p_{ik}^n. \tag{3.10}$$

At this point, however, something appears to be missing. In the original path-integral expression (2.11), the computation at each time layer is sequential: the integrand for u^n contains both $(u^{n+1} - u^n)^2$ and $(u^n - u^{n-1})^2$. Yet the construction of the update scheme in (3.10) uses only one of these terms. A correction is therefore necessary. For an N-fold Gaussian integral we have the exact result:

$$\prod_{n=1}^{N} \left\{ \int_{-\infty}^{\infty} \frac{\mathrm{d}u^n}{\sqrt{2\pi\Delta t}} \exp\Big[- \frac{(u^{n+1} - u^n)^2}{2\Delta t} \Big] \right\} = \frac{1}{\sqrt{N}}. \tag{3.11}$$

Hence, when we iterate the scheme step by step, starting from the second layer ($n = 2$), the update at the n-th layer should be multiplied by a factor $\sqrt{(n-1)/n}$ for correction. Equation (3.10) is thus modified to

$$K_k^{n+1} = \sum_{i=-I}^{I} K_i^n \exp\Big(\frac{1}{2}\omega^2 (u_i^n)^2 \Delta t + \mathrm{i}^{3/2} J(t^n) u_i^n \Delta t\Big)\, p_{ik}^n \sqrt{\frac{n-1}{n}}. \tag{3.12}$$

Moreover, as remarked earlier, the integration at the $n = 0$ layer is fictitious, so the result for the $n = 1$ layer also requires adjustment. Note that at the initial time t^0 the amplitude is non-zero only at the origin $u_0^0 = 0$. Using the formula above, the amplitude at grid point k in the first layer ($n = 1$) becomes

$$K_k^1 = \sum_{i=-I}^{I} K_i^0 \exp\Big(\frac{1}{2}\omega^2 (u_i^0)^2 \Delta t\Big) p_{ik}^0 = K_0^0\, p_{0k}^0. \tag{3.13}$$

On the other hand, the analytic expression for the transition amplitude from the point $u_0^0 = 0$ to u_k^1 after a short time Δt can be derived from (3.17) as

$$K_k^1 = \frac{K_0^0}{\sqrt{\mathrm{i}}} \left[\frac{\Delta u^1}{\sqrt{2\pi\Delta t}} \exp\Big(- \frac{(u_k^1)^2}{2\Delta t} \Big) \right] \frac{1}{\Delta u^1}. \tag{3.14}$$

The term in square brackets can be interpreted as a transition probability. Comparing the two expressions, we see that the numerical computation of the amplitude K_k^1 at the first layer must be divided by the grid spacing Δu^1 of that layer, and the initial condition of K_0^0 needs to be divided by $\sqrt{\mathrm{i}}$ as well.

Following the above procedure, we update the amplitudes iteratively for each time step Δt, thereby completing the evolution from t_0 to T. Finally, if one wishes to compute the transition amplitude at a specific point k, the result is given by (3.12). If the total transition amplitude at time T is desired, as defined in (2.19), we sum over all grid points:

$$\|K^T\| = \left| \sum_{k=-I}^{I} K_k^T \Delta u^T \right|. \tag{3.15}$$

Note the amplitude K is a complex number, its modulus and phase should be computed accordingly.

To validate the stochastic formulation for bosonic fields, we consider a classic example: a one-dimensional harmonic oscillator under a constant external source. The action is given by (2.6) with $J(t) = J_0$ being a constant source. We aim to compute the transition amplitude from $\varphi(0) = a$ to $\varphi(T) = b$:

$$K(b, T; a, 0) = \int \mathcal{D}\varphi \, e^{\mathrm{i}S[\varphi]}. \tag{3.16}$$

For a constant source, this path integral admits a closed-form solution. Following the method presented by Feynman and Hibbs [5], the analytic solution for the case $a = 0$ (i.e., starting from the vacuum state $\varphi = 0$) is

$$\begin{aligned} K(b, T; 0, 0) \;=\; & \sqrt{\frac{\omega}{2\pi \mathrm{i} \, \sin(\omega T)}} \cdot \exp\left\{ \mathrm{i} \frac{b^2 \omega}{2} \frac{\cos(\omega T)}{\sin(\omega T)} \right. \\ & \left. + \mathrm{i} \frac{b J_0}{\omega} \frac{1 - \cos(\omega T)}{\sin(\omega T)} \;+\; \mathrm{i} \frac{J_0^2}{2\omega^3} \left(\omega T - 2 \frac{1 - \cos(\omega T)}{\sin(\omega T)} \right) \right\}. \end{aligned} \tag{3.17}$$

The phase factor in this expression differs slightly from the result given by Feynman and Hibbs. Since this formula is crucial for validating our scheme, a detailed derivation is provided in the Appendix for the reader's reference.

First, we validate the stochastic formulation against analytic solutions for the harmonic oscillator. Figures 3–6 demonstrate perfect agreement for both "closed-path" ($a = b = 0$) and fixed-time evolution scenarios. Notably, Figure 5 reveals that an external source $J_0 > 0$ shifts the amplitude distribution toward $\varphi < 0$, breaking the symmetry observed at $J_0 = 0$. Regarding Figure 6, the observed discontinuities for large J_0 and ω are artifacts of the complex phase's multi-valued nature—purely mathematical features that can be readily handled in numerical implementation, rather than physical phenomena or method errors.

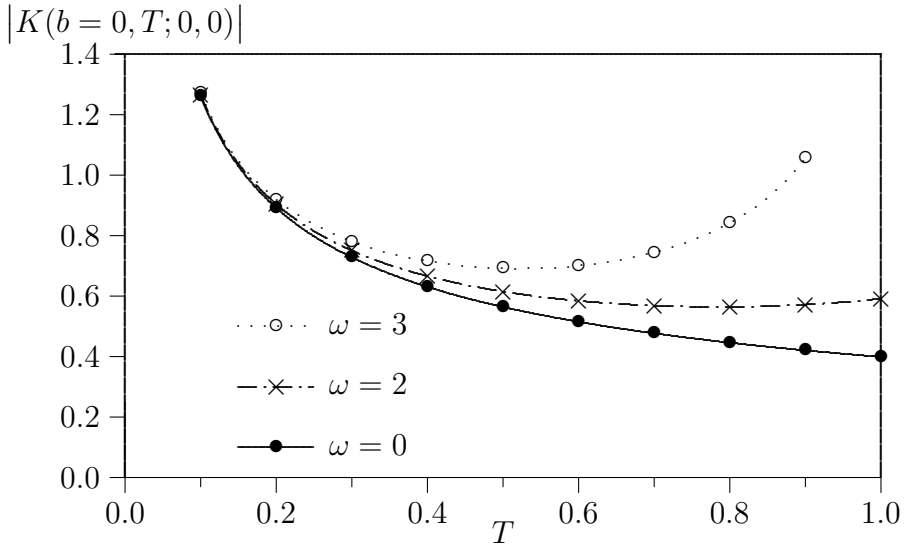

Figure 3: Magnitude of the transition amplitude $|K(b=0,T;0,0)|$ for the forced harmonic oscillator under a constant source. Lines: analytic; symbols: numerical.

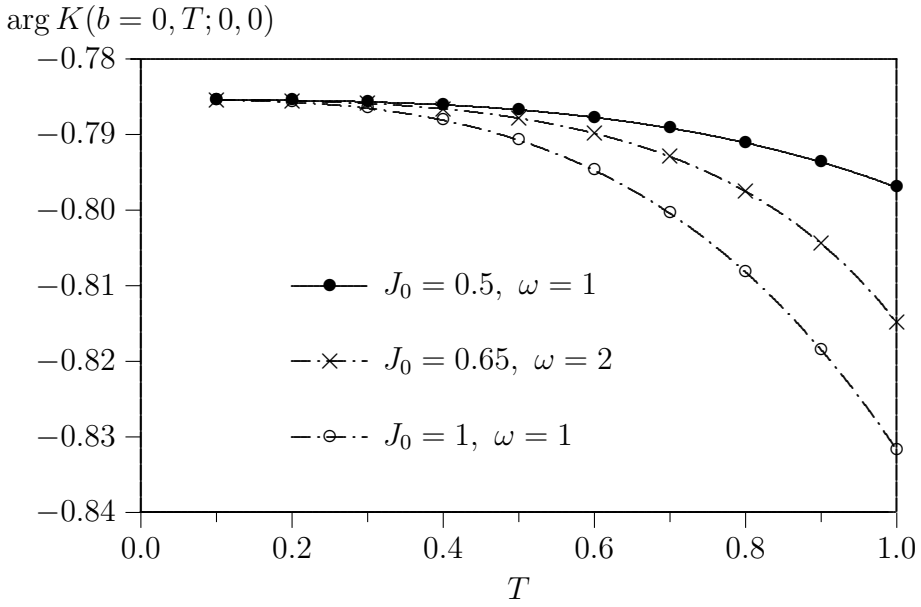

Figure 4: Phase of the transition amplitude $\arg K(b=0,T;0,0)$ for the forced harmonic oscillator under constant source. Lines: analytic; symbols: numerical.

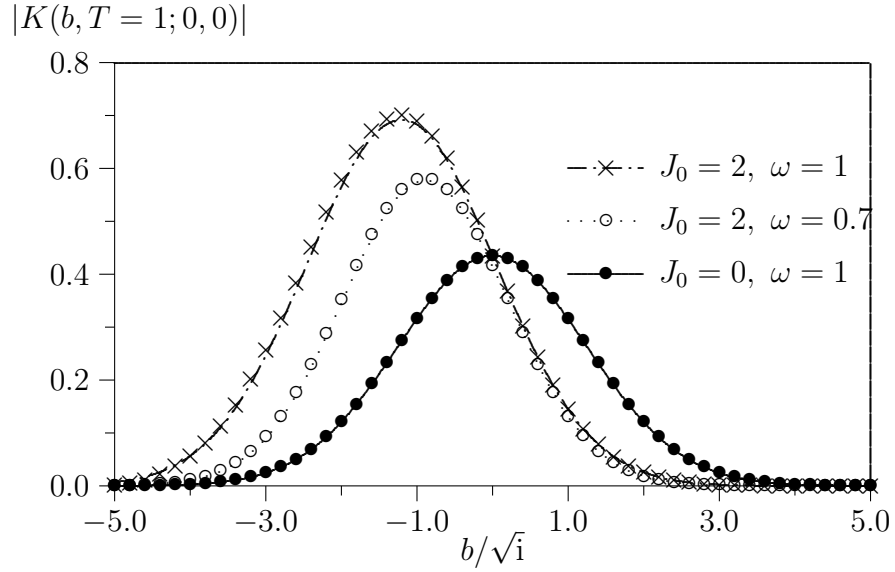

Figure 5: Magnitude of the transition amplitude $|K(b, T = 1; 0, 0)|$ for the forced harmonic oscillator under constant source. Lines: analytic; symbols: numerical.

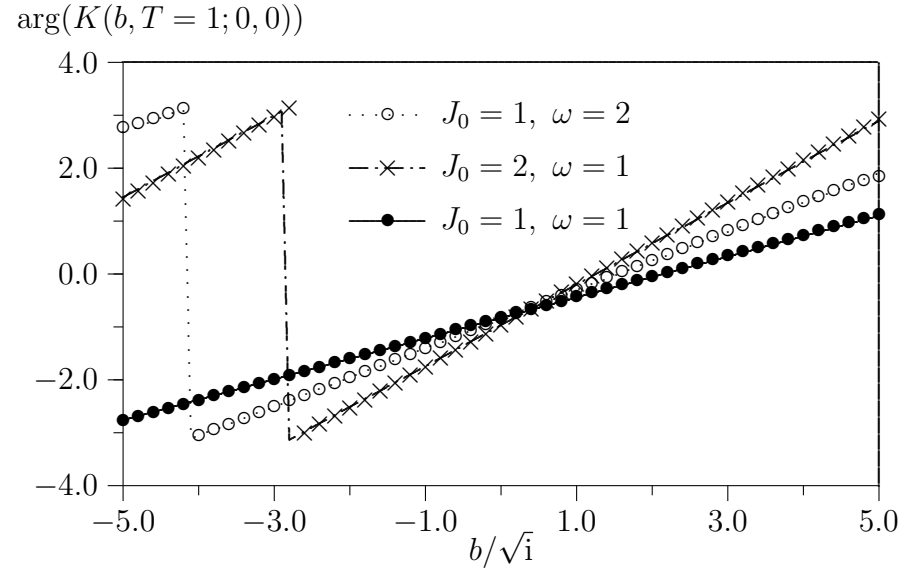

Figure 6: Phase of the transition amplitude $\arg(K(b, T = 1; 0, 0))$ for the forced harmonic oscillator under constant source. Lines: analytic; symbols: numerical.

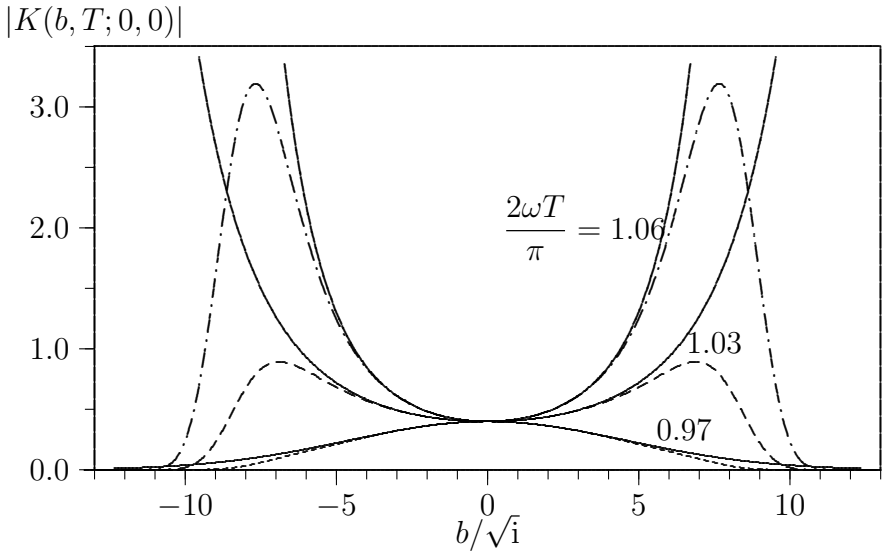

Figure 7: Magnitude of the transition amplitude $|K(b,T;0,0)|$ for the free scalar field harmonic oscillator near the critical time $\omega T = \pi/2$. Solid lines: analytic; dashed or dotted lines: numerical.

However, a critical feature arises in the free massive boson model: the "temporal singularity." As shown in Figure 7, at the critical time $T = \pi/(2\omega)$, the transition amplitude becomes independent of the final state. Consequently, the distribution transforms from bell-shaped to bowl-shaped (bimodal). This singularity effectively bounds the interaction time window for massive bosons.

To address this instability, we examine the ϕ^6 model. The corresponding action, neglecting the external source J (cf. (2.6)), is written as

$$S = \int_{t_0}^{T} \mathrm{d}t \left[\frac{1}{2}\dot{\varphi}^2(t) - \frac{1}{2}\omega^2\varphi^2(t) - \frac{\mu}{6!}\varphi^6(t)\right], \tag{3.18}$$

where μ is the model coefficient. Unlike the free field, the ϕ^6 term introduces a strong damping potential that suppresses large field excitations. As illustrated in Figure 8, this damping prevents the formation of bimodal distributions. For a large μ, even if the amplitude expands initially, it contracts back to the origin, ensuring a stable, bell-shaped distribution suitable for long-term evolution.

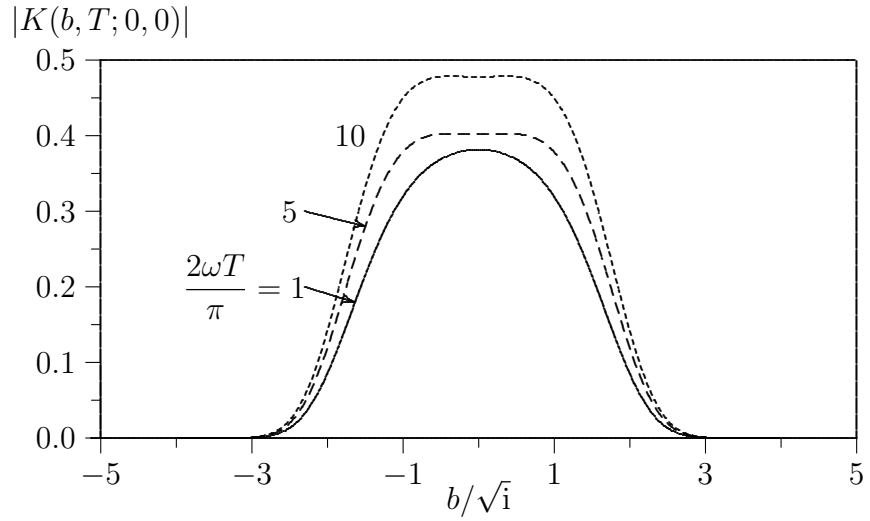

Figure 8: Magnitude of the transition amplitude $|K(b,T;0,0)|$ for the scalar ϕ^6 model at different times T, calculated by the stochastic method with $\mu = 36$.

4 Stochastic formulation of the Dirac field

In quantum field theory, the Lagrangian for a free Dirac spinor field is given by

$$\mathcal{L} = \bar{\psi}\big(\mathrm{i}\gamma^\mu \partial_\mu - \lambda\big)\psi, \tag{4.1}$$

where, for later convenience in modeling with a Poisson process, we denote the spinor-field mass by λ. The Fermion field ψ possesses two spinorial degrees of freedom: a left-handed Weyl field $\psi_L(t,\vec{x})$ and a right-handed Weyl field $\psi_R(t,\vec{x})$, i.e., $\psi = (\psi_L, \psi_R)^T$, both being two-component complex spinors.

To focus on the internal dynamics induced by the mass term, we consider a spatially localized fermionic excitation and replace the spatial dependence with a stochastic variable. This reduces the Weyl fields to time-dependent complex amplitudes $q_L(t), q_R(t) \in \mathbb{C}$. The fields can then be separated as

$$\psi_L(t,\vec{x}) = q_L(t)\, f(\vec{x}), \qquad \psi_R(t,\vec{x}) = q_R(t)\, f(\vec{x}), \tag{4.2}$$

where $f(\vec{x}) \in \mathbb{R}$ is a spherically symmetric, normalized real function satisfying

$$\int_{\mathbb{R}^3} f^2(\vec{x})\, \mathrm{d}^3x = 1, \qquad \int_{\mathbb{R}^3} f(\vec{x})\, \partial_i f(\vec{x})\, \mathrm{d}^3x = 0, \quad (i = 1,2,3). \tag{4.3}$$

After performing the spatial integration, the classical action for the Lagrangian in (4.1) can be written as

$$\begin{aligned} S = \int \mathrm{d}t\mathrm{d}^3x\mathcal{L} &= \int \mathrm{d}t \left[\mathrm{i}q_L^\dagger(t)\dot{q}_L(t) + \mathrm{i}q_R^\dagger(t)\dot{q}_R(t) - \lambda\big(q_L^\dagger(t)q_R(t) + q_R^\dagger(t)q_L(t)\big)\right] \\ &= \int \mathrm{d}t \left[\mathrm{i}q^\dagger(t)\dot{q}(t) - \lambda\, q^\dagger(t)\sigma_1 q(t)\right], \end{aligned} \tag{4.4}$$

where $q(t)$ is a vector, and σ_1 is a matrix:

$$q(t) = \begin{pmatrix} q_L(t) \\ q_R(t) \end{pmatrix}, \qquad \sigma_1 = \begin{pmatrix} 0 & 1 \\ 1 & 0 \end{pmatrix}. \tag{4.5}$$

The corresponding Euler–Lagrange equation of motion to (4.4) is

$$\mathrm{i}\frac{\mathrm{d}}{\mathrm{d}t}\begin{pmatrix} q_L \\ q_R \end{pmatrix} = \lambda\sigma_1 \begin{pmatrix} q_L \\ q_R \end{pmatrix} = \lambda \begin{pmatrix} q_R \\ q_L \end{pmatrix}. \tag{4.6}$$

From this moving equation we can see that the existence of q_L implies a jump to q_R with a factor of amplitude $-\mathrm{i}\lambda\mathrm{d}t$, and the existence of q_R implies a jump to q_L with the same factor. Thus, the underlying physical process is the coherent oscillations between the two components with frequency λ (the quantum-mechanical Zitterbewegung). This exhibits the characteristic Dirac-type dynamics and can simulate the evolution of a fermionic state.

It is worth noting that the bilinear combination

$$j(t) := q^\dagger(t)\sigma_1 q(t) = q_L^\dagger(t)q_R(t) + q_R^\dagger(t)q_L(t) = 2\,\mathrm{Re}(q_L^* q_R) \tag{4.7}$$

is precisely the projection of the scalar density $\psi_L^\dagger\psi_R + \mathrm{h.c.}$ of the original field theory under the localized excitation approximation (4.2):

$$\int \mathrm{d}^3x\ \psi_L^\dagger(t,\vec{x})\psi_R(t,\vec{x}) + \mathrm{h.c.} = j(t). \tag{4.8}$$

Consequently, this structure can also be naturally employed for Yukawa coupling with a scalar field $\varphi(t)$ (e.g., $-g\varphi j$), or as part of a vector current interacting with a gauge field.

We now search for a transition amplitude for the system, namely, a 2×2 matrix $K(\Delta t)$ which makes $q(t)$ transits to

$$q(t+\Delta t) = K(\Delta t)q(t). \tag{4.9}$$

It is known from (4.6) that the transition of $q(t)$ includes not only the continuous evolution of the two components q_L and q_R, but also discrete jumps between these two components. Thus the transition amplitude $K(\Delta t)$ must be applicable both to continuous and jump.

To capture the jump stochastic nature, we model the dynamics as a continuous-time two-state Markov chain. Define a stochastic process $\xi(t) \in \{L, R\}$ that indicates the internal state of the system at time t. The process is driven by Poisson jumps with intensity λ, causing $\xi(t)$ to switch between the two states at random times. The total number of jumps up to time t, denoted by $N(t)$, follows a Poisson distribution:

$$\mathbb{P}(N(t) = n) = \frac{(\lambda t)^n}{n!} e^{-\lambda t}. \tag{4.10}$$

Motivated by the Euler–Lagrange equation (4.6): for a small time step Δt, the amplitude for a transition from q_L to q_R is $-\mathrm{i}\lambda\Delta t + \mathcal{O}(\Delta t^2)$, the leading-order transition amplitude is proportional to $-\mathrm{i}$. To capture this universal phase structure in the stochastic formulation, we assign a factor of $-\mathrm{i}$ to each jump event, while the jump rate λ governs the probability of transitions. The amplitude from an initial state $\xi(0) = \alpha$ to a final state $\xi(t) = \beta$ is defined as the sum over all paths that start at α and end at β, each weighted by $(-\mathrm{i})^{N(t)}$. Motivated by the correspondence between the matrix σ_1 and the state switching, we postulate the following stochastic expectation for the transition amplitude:

$$K_{\beta\alpha}(t) = c\, \mathbb{E}_{\xi(0)=\alpha} \left[(-\mathrm{i})^{N(t)} \cdot \mathbf{1}_{\{\xi(t)=\beta\}} \right], \tag{4.11}$$

where $\mathbf{1}_{\{\xi(t)=\beta\}}$ is the indicator function equal to 1 if $\xi(t) = \beta$ and 0 otherwise. The constant c is fixed by the requirement that the transition amplitude matrix $K(\Delta t)$ be unitary, $K^\dagger K = I$, which implies that each column must have unit norm:

$$\sum_{\beta=L,R} |K_{\beta\alpha}|^2 = 1, \qquad (\text{for } \alpha = L, R). \tag{4.12}$$

Let us consider the evolution from an initial state α to a final state β over a short time interval $\Delta t = t - t_0$. Suppose the process $\xi(t)$ undergoes n jumps during this interval. Because the system has only two states, L and R, an odd number of jumps leads to a transition from α to β, while an even number of jumps returns the system to α (equivalent

to no net transition). The transition amplitudes therefore take the form

$$\begin{aligned} K_{\alpha\alpha}(\Delta t) &= c\sum_{n=0}^{\infty}(-\mathrm{i})^{2n}\frac{(\lambda\Delta t)^{2n}}{(2n)!}e^{-\lambda\Delta t} = c\cos(\lambda\Delta t)e^{-\lambda\Delta t}, \\ K_{\beta\alpha}(\Delta t) &= c\sum_{n=0}^{\infty}(-\mathrm{i})^{2n+1}\frac{(\lambda\Delta t)^{2n+1}}{(2n+1)!}e^{-\lambda\Delta t} = -\mathrm{i}c\sin(\lambda\Delta t)e^{-\lambda\Delta t}. \end{aligned} \tag{4.13}$$

Using (4.12) for the transition process,

$$|K_{\alpha\alpha}(\Delta t)|^2 + |K_{\beta\alpha}(\Delta t)|^2 = (c\,e^{-\lambda\Delta t})^2 = 1, \tag{4.14}$$

which gives $|c| = e^{\lambda\Delta t}$. To fix the phase of c, we require the transition matrix to be unitary and to approach the identity matrix as $\Delta t \to 0$. This leads to the choice $c = e^{\lambda\Delta t}$ (the positive real solution). Consequently, the transition amplitudes become

$$K_{\alpha\alpha}(\Delta t) = \cos(\lambda\Delta t), \qquad K_{\beta\alpha}(\Delta t) = -\mathrm{i}\sin(\lambda\Delta t). \tag{4.15}$$

The complex phase factor $(-\mathrm{i})$ precisely represents the amplitude acquired when $\xi(t)$ jumps between different states.

We now turn to the transition amplitude for continuous evolution. Since the Euler–Lagrange equation (4.6) is a linear first-order differential equation with constant coefficient, its solution,

$$q(t) = e^{-\mathrm{i}Ht}q(0), \qquad H := \lambda\sigma_1, \tag{4.16}$$

defines a linear, unitary and continuous time evolution. This means that the dynamics of the system is fully determined by the initial state and the operator $K(t) = e^{-\mathrm{i}Ht}$. The evolution operator is

$$e^{-\mathrm{i}Ht} = e^{-\mathrm{i}\lambda t\sigma_1} = \sum_{k=0}^{\infty}\frac{1}{k!}(-\mathrm{i}\lambda t)^k\sigma_1^k = \cos(\lambda t)\,I - \mathrm{i}\sin(\lambda t)\,\sigma_1, \tag{4.17}$$

which exactly reproduces the amplitudes (4.15) obtained from the Poisson process. Thus, for both continuous and jump evolution, we have the transition amplitude matrix which, similar to the Boson scalar field case, also defines an evolution operator as

$$q(t+\Delta t) = \mathbb{K}(\Delta t)q(t) = \begin{pmatrix} \cos(\lambda\Delta t) & -\mathrm{i}\sin(\lambda\Delta t) \\ -\mathrm{i}\sin(\lambda\Delta t) & \cos(\lambda\Delta t) \end{pmatrix} q(t). \tag{4.18}$$

Notably, this formulation achieves the unitary evolution of the spinor field using only complex numbers and Poisson statistics, completely bypassing the need for anti-commuting Grassmann variables.

5 Numerical scheme for the Dirac field

Based on the Poisson stochastic formulation of the spinor-field path integral, we now propose a corresponding numerical finite-difference scheme, enabling computer simulations of fermionic evolution in quantum field theory. This section examines a simple yet typical model: computing the physical transition probability $\mathbb{P}_{L\to R}$ for a two-state fermion under the influence of a classical scalar field $\phi_{\rm cl}(t)$ from the left-handed state $|L\rangle$ to the right-handed state $|R\rangle$, and comparing the result with perturbation theory in the weak-coupling regime ($g \ll 1$).

We assume that the scalar field is non-dynamical, modeled as a Gaussian pulse of a massless boson occurring at $t = 0$:

$$\phi_{\rm cl}(t) = e^{-t^2/(2\tau^2)}, \qquad \text{with } \tau = 1. \tag{5.1}$$

The Yukawa-type coupling term $-g\phi_{\rm cl} j$ corresponds in this model to the Lagrangian

$$\mathcal{L} \;=\; \mathrm{i} q^\dagger(t)\dot{q}(t) - g\phi_{\rm cl}(t)\, q^\dagger(t)\sigma_1 q(t), \tag{5.2}$$

where we assume that the fermion is massless (i.e., no $\lambda\, q^\dagger\sigma_1 q$ term) and the scalar field $\phi_{\rm cl}(t)$ is a prescribed classical external field. According to standard time-dependent perturbation theory [1], for this simple model, the first-order transition probability is given by

$$\mathbb{P}^{\rm pert}_{L\to R} = 2\pi g^2. \tag{5.3}$$

Following the stochastic formulation for the spinor field established in Section 4, we treat the evolution of this system as a continuous-time two-state Markov chain. Define an effective coupling strength

$$\lambda(t) = g\,\phi_{\rm cl}(t), \tag{5.4}$$

then we can use (4.18) to perform the evolution.

We choose a sufficiently large number T to define the time interval $[-T, T]$ over which the evolution is simulated. We then discretize this interval into $2N$ equal time steps of length $\Delta t = T/N$, i.e.,

$$t^n = -T + n\Delta t, \qquad (n = 0, 1, \cdots, 2N). \tag{5.5}$$

Thus, we obtain the explicit finite-difference scheme:

$$\begin{aligned} q_L^{n+1} &= \cos(\lambda^n \Delta t)\, q_L^n - \mathrm{i} \sin(\lambda^n \Delta t)\, q_R^n, \\ q_R^{n+1} &= \cos(\lambda^n \Delta t)\, q_R^n - \mathrm{i} \sin(\lambda^n \Delta t)\, q_L^n, \end{aligned} \tag{5.6}$$

where $\lambda^n = g\, \phi_{\mathrm{cl}}(t^n)$, and the initial conditions are

$$q_L^0 = 1, \qquad q_R^0 = 0. \tag{5.7}$$

After $2N$ iterations we obtain the final state $q^{2N} = (q_L^{2N}, q_R^{2N})^T$. The physical transition probability from the left-handed state $|L\rangle$ to the right-handed state $|R\rangle$ is then given by the squared modulus of the amplitude on $|R\rangle$:

$$\mathbb{P}_{L\to R}^{\mathrm{num}} = \left| q_R^{2N} \right|^2. \tag{5.8}$$

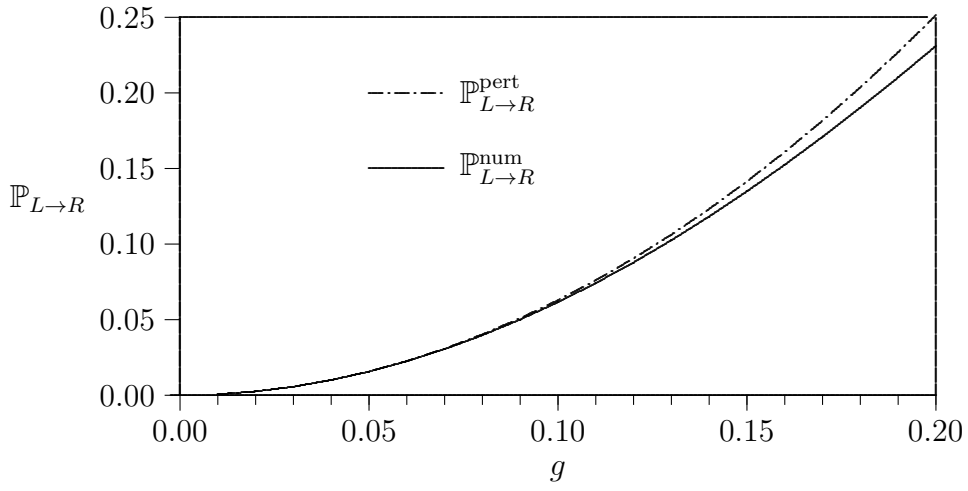

Figure 9: The transition probability of a Fermion from left-hand state to right-hand state.

Regarding numerical stability, the von Neumann analysis confirms that scheme (5.6) is unconditionally stable. However, to properly resolve the evolution of $\lambda(t)$ and avoid

approximation errors, a sufficiently small time step is required. We perform simulations with $\Delta t = 0.001$ and integration limit $T = 10$, which effectively captures the dynamics over the entire real line. As shown in Figure 9, the numerical results align excellently with first-order perturbation theory (5.3) in the weak-coupling regime, validating the accuracy of the stochastic method.

6 Yukawa model and calculation of fermion mass

We now consider the case where a bosonic scalar field φ and a fermionic spinor field $q = (q_L, q_R)^T$ are coupled through the Yukawa model. Following the variable notation established in the preceding chapters, the Lagrangian of the system is expressed as

$$\mathcal{L} = \frac{1}{2}\dot{\varphi}^2 - \frac{1}{2}\omega^2\varphi^2 \,+\, \mathrm{i}q^\dagger\dot{q} - \lambda\, q^\dagger\sigma_1 q \,-\, g\,\varphi\, q^\dagger\sigma_1 q. \tag{6.1}$$

where g is the Yukawa coupling constant. From a physical perspective, the Yukawa term plays a dual role: on one hand, it serves as the coupling between the fermionic internal transition $(q^\dagger\sigma_1 q)$ and the bosonic field, providing an effective external source $J = -g(q^\dagger\sigma_1 q)$ for the φ field, thereby driving the distribution of the φ field away from its symmetric center; on the other hand, this asymmetric distribution of the φ field feeds back onto the fermion, correcting its effective mass from the initial mass λ to $\lambda + g\varphi$, which in turn modulates the transition frequency between the two components of the fermion. This section aims to demonstrate the applicability of the stochastic formulation in handling nonlinear and non-perturbative problems by calculating the dynamical evolution of the effective mass λ_{eff} of the fermionic q field during the coupling process.

Let the joint transition amplitude of the system be $K = K^{\varphi,q}$, whose evolution from t_0 to T can be expressed using the Feynman path integral as

$$K^{\varphi,q} = \int \mathcal{D}\varphi\,\mathcal{D}q\,\exp\left\{\mathrm{i}\int_{t_0}^{T}\left(\frac{1}{2}\dot{\varphi}^2 - \frac{1}{2}\omega^2\varphi^2 \,+\, \mathrm{i}q^\dagger\dot{q} - \lambda\, q^\dagger\sigma_1 q \,-\, g\,\varphi\, q^\dagger\sigma_1 q\right)\right\}. \tag{6.2}$$

Within the framework of the stochastic formulation, this joint transition amplitude can be decomposed into an iterative form of conditional evolutions:

$$\begin{aligned} K^{\varphi,q}(t^{n+1}) \;\;=\;\; \mathbb{K}^{u,N}\left[\exp\left(-\frac{\mathrm{i}}{2}\omega^2\varphi^2\,\Delta t\right)\cdot(-\mathrm{i})^{N(\Delta t)}\cdot\exp\left(-\mathrm{i}g\varphi j\,\Delta t\right)\Big|\, t^n\right]\, K^{\varphi,q}(t^n), \\ (n = 0, 1, \cdots), \end{aligned} \tag{6.3}$$

where $u = \mathrm{i}^{-1/2}\varphi$ is the Wiener process, $N(\Delta t)$ is the total number of internal transitions of the q field within the time interval Δt, following a Poisson process with intensity λ, and $j = q^\dagger \sigma_1 q$ is the transition current intensity of the fermionic field.

Since the q field is a two-dimensional spinor, the above equation is essentially a 2×2 matrix equation. Introducing the wave function vector

$$f(t;\varphi) = f_L(t;\varphi)|L\rangle + f_R(t;\varphi)|R\rangle = \begin{pmatrix} f_L(t;\varphi) \\ f_R(t;\varphi) \end{pmatrix}, \tag{6.4}$$

the equation can be rewritten in terms of two components:

$$\begin{aligned} f(t^{n+1};\varphi) &= \mathbb{K}^{u,N}\left[\exp\Big(-\frac{\mathrm{i}}{2}\omega^2\varphi^2\,\Delta t\Big)\cdot(-\mathrm{i})^{N(\Delta t)}\cdot\exp\Big(-\mathrm{i}g\varphi j\,\Delta t\Big)\,\Big|\,t^n\right] f(t^n;\varphi), \\ & \qquad (n = 0, 1, \cdots). \end{aligned} \tag{6.5}$$

To numerically implement the above evolution, we adopt the Strang splitting scheme [9], dividing each time step $[t^n, t^{n+1}]$ into two sub-steps:

$$\begin{aligned} f(t^{n+1/2};\varphi) &= \mathbb{K}^{u}\left[\exp\Big(\frac{1}{2}\omega^2 u^2\,\Delta t\Big)\cdot\exp\Big(-\mathrm{i}^{3/2}guj\,\Delta t\Big)\,\Big|\,t^n\right] f(t^n;\varphi), \\ f(t^{n+1};\varphi) &= \mathbb{K}^{N}\left[(-\mathrm{i})^{N(\Delta t)}\cdot\exp\Big(-\mathrm{i}g\varphi j\,\Delta t\Big)\,\Big|\,t^n\right] f(t^{n+1/2};\varphi). \end{aligned} \tag{6.6}$$

The first evolution operator $\mathbb{K}^u$ acts on the two components f_L and f_R of f, modifying only their distribution along the φ dimension without altering the relative relationship between the two components. It is worth noting that the external source j here differs from the fixed external source J in Section 3, as it is dynamically determined by the wave function $f(t^n;\varphi)$ at the current time step:

$$j = f^\dagger \sigma_1 f = f_L^* f_R + f_R^* f_L = 2\mathrm{Re}(f_L^* f_R), \tag{6.7}$$

In this calculation we focus on the coupling between a free fermion and a free boson. Both fields are initially symmetric. Thus, we choose the initial condition as

$$f(0;0) = \begin{pmatrix} f_L(0;0) \\ f_R(0;0) \end{pmatrix} = \frac{1}{\sqrt{2}}\begin{pmatrix} 1+0\mathrm{i} \\ 1+0\mathrm{i} \end{pmatrix}, \tag{6.8}$$

while setting $f(0;\varphi) = 0$ for $\varphi \neq 0$. Since $\mathbb{K}^u$ applies the same evolution to both components and $\mathbb{K}^N$ is a unitary operator, it is guaranteed that f_L and f_R remain equal throughout the evolution.

It should be noted that, due to the presence of the interaction term, the independent action of the evolution operator $\mathbb{K}^u$ on the two components does not automatically guarantee the physical probability conservation. Therefore, after each sub-step is completed, the wave function f must be explicitly normalized. Following the physical probability calculation rule defined in the previous sections (see (2.19) and (4.12)), we define the normalization factor $\|f(t)\|$ as the modulus of the integrated spinor components:

$$\|f(t)\| := \sqrt{\Big|\sum_k f_L(t;\varphi_k)\Delta\varphi_k\Big|^2 + \Big|\sum_k f_R(t;\varphi_k)\Delta\varphi_k\Big|^2}. \tag{6.9}$$

Subsequently, the evolved distribution $f(t^{n+1/2};\varphi)$ is divided by this factor $\|f(t^{n+1/2})\|$ to satisfy the normalization condition $\|f\| = 1$.

The second evolution operator $\mathbb{K}^N$ corresponds to the 2×2 matrix evolution established in Section 4, which performs internal mixing of $f(t^{n+1/2};\varphi_k)$ at each fixed φ_k without altering its distribution along the φ dimension. The specific form is given by

$$f(t^{n+1};\varphi) = \begin{pmatrix} \cos(\lambda_\varphi \Delta t) & -\mathrm{i}\sin(\lambda_\varphi \Delta t) \\ -\mathrm{i}\sin(\lambda_\varphi \Delta t) & \cos(\lambda_\varphi \Delta t) \end{pmatrix} f(t^{n+1/2};\varphi), \tag{6.10}$$

where the effective frequency λ_φ is given by the Lagrangian (6.1):

$$\lambda_\varphi = \lambda + g\varphi. \tag{6.11}$$

From this, it can be seen that the bosonic field φ modulates the effective mass of the fermion through its symmetry. At points where $\varphi > 0$, λ_φ increases, while at points where $\varphi < 0$, λ_φ decreases.

After evolving the wave function via $\mathbb{K}^N$ at a specific point φ, we calculate the fermionic current j to drive the evolution of the φ field in the subsequent time step. According to (6.7),

$$j(t^{n+1};\varphi) = f(t^{n+1};\varphi)^\dagger \sigma_1 f(t^{n+1};\varphi) =: J(\varphi). \tag{6.12}$$

Since j depends on φ, we decompose it into even and odd components for analysis:

$$j(t^{n+1};\varphi) := J_+(\varphi) + J_-(\varphi) = \frac{1}{2}\big(J(\varphi) + J(-\varphi)\big) + \frac{1}{2}\big(J(\varphi) - J(-\varphi)\big). \tag{6.13}$$

Based on the results in Figure 5 (Section 3), the even current J_+ modulates the shape of the φ distribution: $J_+ < 0$ (implying a force $-gJ_+ > 0$) pushes the field toward the $\varphi \le 0$

region, whereas $J_+ > 0$ pushes it toward $\varphi \geq 0$. Conversely, the odd current J_- couples to the bosonic mass term ω^2, effectively scaling the width of the distribution: $J_- < 0$ leads to an expansion, while $J_- > 0$ results in a contraction. Thus, the influence of the fermionic current j on the bosonic field is distinctly characterized by these two mechanisms.

Similar to the first step of $\mathbb{K}^u$ evolution, after completing the $\mathbb{K}^N$ evolution for all φ points, the wave function f must also be normalized to ensure overall physical probability conservation.

Next, we discuss the calculation of the fermion mass. When a fermion is coupled to a scalar field through the Yukawa term, its initial mass λ changes to an effective mass λ_{eff}. The mass shift is defined as

$$\delta\lambda(t) = \lambda_{\text{eff}} - \lambda. \tag{6.14}$$

After each time step t^n is completed, we take the expectation of $f(t^n, \varphi)$ along the φ dimension, yielding

$$\bar{f}^n = \int_{-\infty}^{\infty} f(t^n;\varphi)\mathrm{d}\varphi = \sum_k f(t^n;\sqrt{\mathrm{i}}u_k^n)\,\sqrt{\mathrm{i}}\Delta u_k^n. \tag{6.15}$$

Assuming that the evolution from $\bar{f}^n$ to $\bar{f}^{n+1}$ is governed by some effective mass λ^n, the evolution operator gives

$$\begin{aligned} \bar{f}_L^{n+1} &= \cos(\lambda^n\Delta t)\bar{f}_L^n - \mathrm{i}\sin(\lambda^n\Delta t)\bar{f}_R^n, \\ \bar{f}_R^{n+1} &= \cos(\lambda^n\Delta t)\bar{f}_R^n - \mathrm{i}\sin(\lambda^n\Delta t)\bar{f}_L^n. \end{aligned} \tag{6.16}$$

Since the two components of $\bar{f}^n$ are always equal, $\bar{f}_R^n = \bar{f}_L^n$, hence

$$\bar{f}_L^{n+1}/\bar{f}_L^n = \cos(\lambda^n\Delta t) - \mathrm{i}\sin(\lambda^n\Delta t) = e^{-\mathrm{i}\lambda^n\Delta t}, \tag{6.17}$$

which yields the calculation formula for the effective mass

$$\lambda^n = \frac{1}{\Delta t}\arg\Big(\frac{\bar{f}_L^n}{\bar{f}_L^{n+1}}\Big). \tag{6.18}$$

Correspondingly, the mass shift is given by

$$\delta\lambda(t^n) = \frac{1}{\Delta t}\arg\Big(\frac{\bar{f}_L^n}{\bar{f}_L^{n+1}}\Big) - \lambda. \tag{6.19}$$

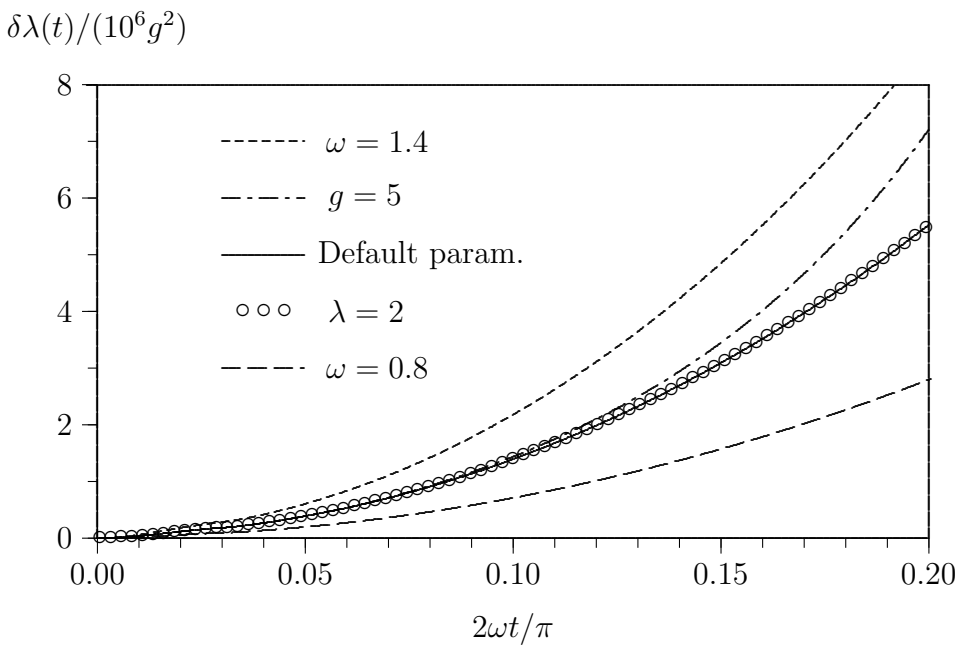

Figure 10: Early-time fermion mass shift $\delta\lambda/(10^6 g^2)$ in the Yukawa model compared to first-order perturbation theory. Default parameters: $g = 1$, $\omega = 1$, $\lambda = 1$.

For comparison, classical perturbative quantum field theory provides the analytical expression for the mass shift under the one-loop approximation [10, 11]:

$$\delta\lambda_c(g, \omega, \lambda) = \frac{g^2\lambda}{4\pi} \int_0^1 (1 - x) \ln\Big[1 - x + \Big(\frac{\omega}{\lambda}\Big)^2 x^2\Big]\, dx. \tag{6.20}$$

This expression indicates that in the weak-coupling regime, the mass shift is proportional to g^2, with its magnitude and sign determined by the ratio ω/λ.

In the following, we present the fermionic mass shift calculations using the stochastic method and compare them with perturbative results. Due to the significant variation of the mass shift during evolution, we discuss it in two stages.

The first stage corresponds to the initial evolution ($0 \leq 2\omega t/\pi \leq 0.2$). As shown in Figure 10, the mass shift $\delta\lambda$ initially exhibits a strict g^2 scaling, consistent with perturbation theory (6.20). However, as time progresses, deviations arise due to higher-order g contributions—a feature inaccessible to perturbative methods. Furthermore, $\delta\lambda$ shows a polynomial dependence on the boson mass ω but is independent of the initial fermion mass λ. This independence contrasts sharply with perturbation theory and stems from the fact that the field deformation is driven by the fermionic flux j, which depends on the transition amplitude

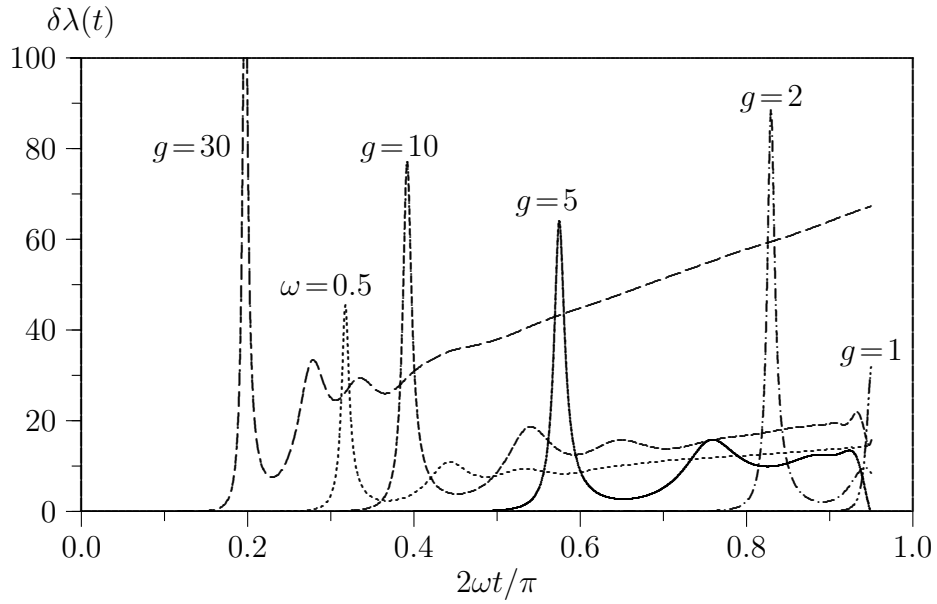

Figure 11: Long-time evolution of the fermion mass shift $\delta\lambda$ in the Yukawa model. Default parameters: $g = 5$, $\omega = 1$, $\lambda = 1$.

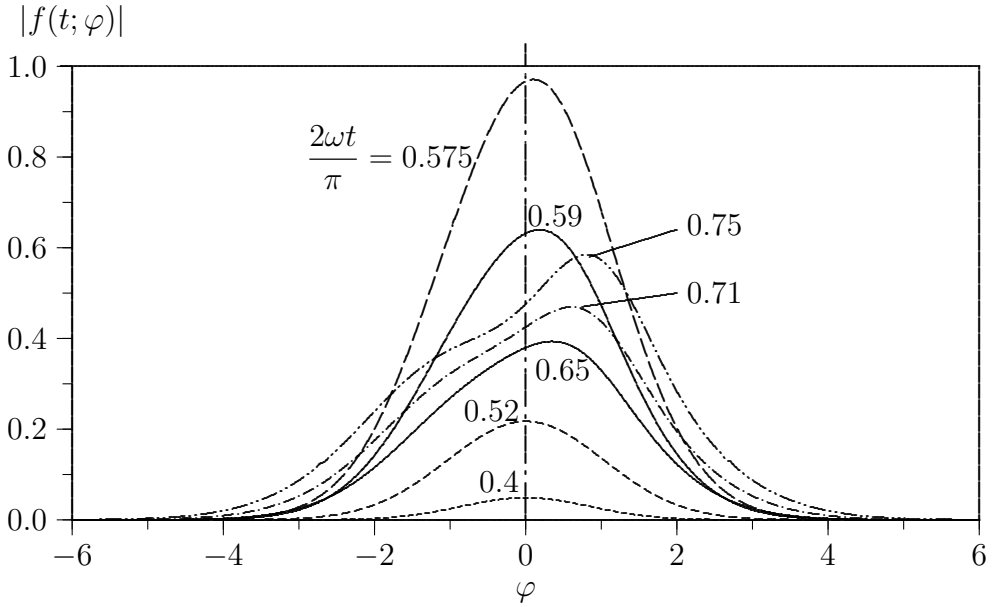

Figure 12: Wave function distribution $|f(t;\varphi)|$ at different times t in the Yukawa model. Parameters: $g = 5$, $\omega = 1$, $\lambda = 1$.

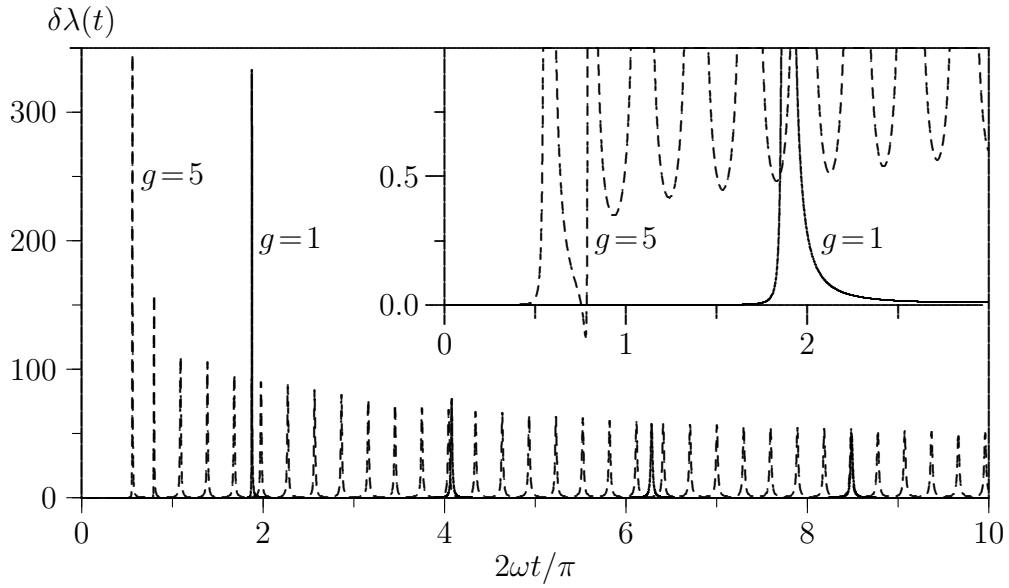

Figure 13: Long-time evolution of the fermion mass shift $\delta\lambda$ in the Yukawa model coupled to a ϕ^6 scalar field. Common parameters: $\omega = 1$, $\lambda = 1$, $\mu = 36$, and $g = 1$ (solid), $g = 5$ (dashed).

rather than λ directly.

The second stage ($0.2 \leq 2\omega t/\pi \leq 1$) covers the intermediate evolution where $\delta\lambda$ exhibits a local peak (Figure 11). This behavior reflects the dynamical coupling mechanism: the rise and fall of $\delta\lambda$ accompany the expansion and contraction of the field distribution (Figure 12). The peak timing is primarily governed by g and ω: a larger g (stronger coupling) or smaller ω (weaker restoring force) leads to an earlier peak.

Beyond this intermediate stage ($2\omega t/\pi \geq 1$), the free boson evolution encounters a time singularity. However, as discussed in Section 3, introducing a ϕ^6 term can avoid this singularity and stabilize the evolution. Figure 13 demonstrates that with the ϕ^6 term, the mass shift tends toward a periodic oscillation pattern, with frequency related to g. This suggests that the ϕ^6 model provides a viable theoretical framework for describing massive bosons that couple stably with fermions over long durations.

7 QED model and gauge interaction

Having validated the method on the scalar Yukawa interaction, we now extend the framework to the vector coupling present in QED. In quantum field theory, the Lagrangian of the QED model is given by

$$\mathcal{L} = \frac{1}{2}\big(\dot{\vec{A}}^2 - (\nabla \times \vec{A})^2\big) + \bar{\psi}\big(\mathrm{i}\gamma^0\partial_t + \mathrm{i}\vec{\gamma}\cdot\nabla - \lambda\big)\psi - \bar{\psi}\big(\hat{e}\gamma^\mu A_\mu\big)\psi. \tag{7.1}$$

To demonstrate the feasibility of the stochastic method in handling gauge interactions, we adopt a simplified "toy model" scenario via local excitation in field space. We replace the spatial coordinate dependence with a dependence on random variables. Assuming the spatial variation is concentrated near the origin, we decompose the fields into time-dependent amplitudes and a fixed spatial profile:

$$\begin{aligned} \vec{A}(t,\vec{x}) &= \big(\varphi_1(t),\varphi_2(t),\varphi_3(t)\big)^T F(\vec{x}), \\ \psi(t,\vec{x}) &= \big(q_L(t),q_R(t)\big)^T F(\vec{x}), \end{aligned} \tag{7.2}$$

where

$$F(\vec{x}) = \frac{(2\kappa)^{3/2}}{\sqrt{4\pi}} e^{-\kappa r} \tag{7.3}$$

is a normalized, real, spherically symmetric function. Consequently, the kinetic and mass terms are reduced to effective quantum mechanical forms:

$$\frac{1}{2}\int_{\mathbb{R}} \mathrm{d}^3x\,\big(\dot{\vec{A}}^2 - (\nabla\times\vec{A})^2\big) = \frac{1}{2}\Big(\dot{\varphi}_1^2 + \dot{\varphi}_2^2 + \dot{\varphi}_3^2\Big) - \kappa^2\Big(\varphi_1^2+\varphi_2^2+\varphi_3^2\Big), \tag{7.4}$$

$$\int_{\mathbb{R}} \mathrm{d}^3x\,\bar{\psi}\big(\mathrm{i}\gamma^0\partial_t + \mathrm{i}\vec{\gamma}\cdot\nabla - \lambda\big)\psi = \mathrm{i}q^\dagger\dot{q} - q^\dagger\big(\lambda\sigma_1\big)q, \tag{7.5}$$

$$\int_{\mathbb{R}} \mathrm{d}^3x\,\bar{\psi}\big(\hat{e}\gamma^\mu A_\mu\big)\psi = \sqrt{\frac{8\kappa^3}{\pi}}\hat{e}\,q^\dagger\Big(\varphi_0\sigma_0 + \varphi_1\sigma_1 + \varphi_2\sigma_2 + \varphi_3\sigma_3\Big)q. \tag{7.6}$$

In the above equations, σ_μ represent the standard Pauli matrices (with σ_0 as the identity):

$$\sigma_0 = \begin{pmatrix}1&0\\0&1\end{pmatrix}, \quad \sigma_1 = \begin{pmatrix}0&1\\1&0\end{pmatrix}, \quad \sigma_2 = \begin{pmatrix}0&-\mathrm{i}\\\mathrm{i}&0\end{pmatrix}, \quad \sigma_3 = \begin{pmatrix}1&0\\0&-1\end{pmatrix}. \tag{7.7}$$

Let us replace ω^2 with $2\kappa^2$ (setting $\kappa^2 = 0$ for massless photons) to match the single-boson Yukawa model, and introduce an effective charge $e = \sqrt{8\kappa^3/\pi}\hat{e}$. The resulting effective action reads:

$$S = \int \mathrm{d}^4x\mathcal{L} \;=\; \int_{t_0}^{t} \mathrm{d}t\Big[\frac{1}{2}\Big(\dot{\varphi}_1^2 + \dot{\varphi}_2^2 + \dot{\varphi}_3^2\Big) - \frac{\omega^2}{2}\Big(\varphi_1^2 + \varphi_2^2 + \varphi_3^2\Big) + \mathrm{i}q^\dagger\dot{q} - q^\dagger\big(\lambda\sigma_1\big)q - eq^\dagger\Big(\varphi_1\sigma_1 + \varphi_2\sigma_2 + \varphi_3\sigma_3\Big)q\Big]. \tag{7.8}$$

Here, we have employed the radiation gauge ($\nabla \cdot \vec{A} = 0$) to eliminate the non-dynamical component φ_0 (which enforces Gauss's Law). This simplification allows us to focus on the transverse degrees of freedom. While this Abelian toy model serves as a proof of concept, the strategy of isolating dynamical variables via gauge fixing provides a necessary foundation for extending this stochastic framework to non-Abelian gauge fields, such as SU(2) and SU(3), in future work.

Now we define a joint distribution wavefunction vector

$$f(t;\vec{\varphi}) = \begin{pmatrix} f_L(t;\vec{\varphi}) \\ f_R(t;\vec{\varphi}) \end{pmatrix}, \tag{7.9}$$

to describe the evolution of the fermionic field q, where $\vec{\varphi} = (\varphi_1, \varphi_2, \varphi_3)^T$. Based on Eq. (7.8), the Euler-Lagrange dynamical equation for $f(t;\vec{\varphi})$ is given by

$$\mathrm{i}\dot{f} = \Big[(\lambda + e\varphi_1)\sigma_1 + e\varphi_2\sigma_2 + e\varphi_3\sigma_3\Big]f = (\vec{h}\cdot\vec{\sigma})f, \tag{7.10}$$

where $\vec{h} = (\lambda + e\varphi_1, e\varphi_2, e\varphi_3)^T$ and $\vec{\sigma} = (\sigma_1, \sigma_2, \sigma_3)^T$. Within the framework of the stochastic formulation, the evolution equation for f reads

$$f(t+\Delta t;\vec{\varphi}) = \mathbb{K}^f[f(t;\vec{\varphi})] = e^{-\mathrm{i}(\vec{h}\cdot\vec{\sigma})\Delta t}f(t;\vec{\varphi}). \tag{7.11}$$

Expanding $e^{-\mathrm{i}(\vec{h}\cdot\vec{\sigma})\Delta t}$ using Taylor's formula yields

$$e^{-\mathrm{i}(\vec{h}\cdot\vec{\sigma})\Delta t} = \cos(\Omega\Delta t)\sigma_0 - \mathrm{i}\frac{\sin(\Omega\Delta t)}{\Omega}(\vec{h}\cdot\vec{\sigma}), \tag{7.12}$$

where

$$\Omega = |\vec{h}| = \sqrt{(\lambda + e\varphi_1)^2 + (e\varphi_2)^2 + (e\varphi_3)^2}. \tag{7.13}$$

Consequently, by substituting σ_μ into Eq. (7.12), we obtain the matrix form of the evolution equation for f:

$$f(t+\Delta t;\vec{\varphi}) = \begin{pmatrix} \cos(\Omega\Delta t) - \mathrm{i}\dfrac{h_3}{\Omega}\sin(\Omega\Delta t) & -\mathrm{i}\dfrac{h_1 - \mathrm{i}h_2}{\Omega}\sin(\Omega\Delta t) \\ -\mathrm{i}\dfrac{h_1 + \mathrm{i}h_2}{\Omega}\sin(\Omega\Delta t) & \cos(\Omega\Delta t) + \mathrm{i}\dfrac{h_3}{\Omega}\sin(\Omega\Delta t) \end{pmatrix} f(t;\vec{\varphi}). \tag{7.14}$$

This evolution form, describing the coupling of one fermion to multiple bosons, not only encompasses the transverse photon interactions (φ_1, φ_2) in QED but also naturally incorporates the modulation of chiral asymmetry by the longitudinal component φ_3. More importantly, this structure shares an identical algebraic structure with the isospin space of SU(2) gauge fields, laying a direct mathematical foundation for future extensions to the electroweak unified theory.

Within the framework of the stochastic formulation, the evolution of the three bosons φ_1, φ_2, and φ_3 can be simulated using three mutually independent Brownian motions. Following the application of the stochastic formulation in the Yukawa model, we employ a tree-grid method to solve for the evolution operators of the three bosons:

$$\begin{aligned} f(t+\Delta t;\vec{\varphi}+\Delta\varphi_k) &= \mathbb{K}^{\varphi}\left[\exp\Big(-\frac{1}{2}\omega^2\varphi_k^2\,\Delta t\Big)\cdot\exp\Big(-\mathrm{i}e\,\varphi_k j_k\,\Delta t\Big)\,\Big|\,t^n\right] f(t;\vec{\varphi}), \\ &\qquad (k=1,2,3). \end{aligned} \tag{7.15}$$

Here, the intensities of the three fermion-coupled currents are given by

$$\begin{aligned} j_1 &= f^\dagger\sigma_1 f = 2\,\mathrm{Re}\big(f_L^* f_R\big), \\ j_2 &= f^\dagger\sigma_2 f = 2\,\mathrm{Im}\big(f_L^* f_R\big), \\ j_3 &= f^\dagger\sigma_3 f = f_L^* f_L - f_R^* f_R. \end{aligned} \tag{7.16}$$

Thus, Eqs. (7.14) and (7.15) together constitute the evolution scheme for the entire QED system, which can be solved numerically using the Strang splitting scheme [9].

As a numerical example, we employ the stochastic formulation model of QED described above to calculate the dynamic flip probability of a fermionic electron between left-handed and right-handed states under the influence of massless bosonic photons. The calculation parameters are chosen as follows: photon mass $\omega = 0$, fermion mass $\lambda = 1$, and coupling

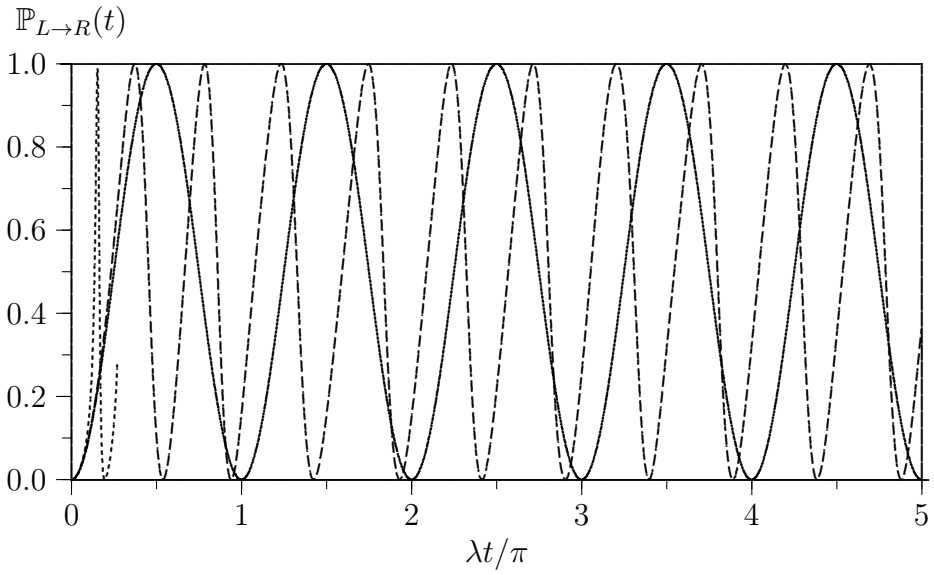

Figure 14: The dynamic transition probability of the Fermion from left-hand state to right-hand state. Parameter: $\omega = 0$, $\lambda = 1$; solid line: Yukawa model $g = 1, 5$; dashed line: QED model $e = 1$; dotted line: QED model $e = 5$.

constant $e = 1$. These results are compared with those of a single-boson Yukawa model with parameter $g = 1$.

The initial conditions at $t = 0$ and at the origin $\vec{\varphi} = 0$ are set as

$$f_L(t = 0; \vec{\varphi} = 0) = 1, \quad f_R(t = 0; \vec{\varphi} = 0) = 0. \tag{7.17}$$

At all other points where $\vec{\varphi} \neq 0$, we have $f_L(t = 0; \vec{\varphi}) = f_R(t = 0; \vec{\varphi}) = 0$.

The physical flip probability we aim to calculate is the squared modulus of the right-handed component of the wavefunction, given by

$$\mathbb{P}_{L\to R}(T) = \left| \int_{-\infty}^{\infty} f_R(T; \vec{\varphi})\, \mathrm{d}\varphi_1 \mathrm{d}\varphi_2 \mathrm{d}\varphi_3 \right|^2. \tag{7.18}$$

In the weak-coupling and short-time limit, second-order perturbation theory predicts a linear growth for the average flip probability:

$$\mathbb{P}^{\mathrm{pert}}_{L\to R}(T) \approx C\, \hat{e}^2\, T. \tag{7.19}$$

where C depends on the boson number. Unlike perturbation theory, the stochastic formulation imposes no restrictions on e or T. While massive bosons ($\omega > 0$) exhibit a temporal

singularity at $T = 2\pi/\omega$, massless photons ($\omega = 0$) do not, allowing for a complete description of the time evolution.

Figure 14 compares the stochastic flip probability $\mathbb{P}_{L\to R}(t)$ with the single-boson Yukawa model. In the Yukawa model, symmetry constraints imply that the fermion-induced current j_1 vanishes. Consequently, the bosonic field remains undisturbed, and the right-handed component integrates to:

$$q_R(\Delta t) = \int_{-\varphi_{\max}}^{\varphi_{\max}} f_R(\Delta t;\varphi)\mathrm{d}\varphi = \int_{-\varphi_{\max}}^{\varphi_{\max}} -\mathrm{i}\sin\Big[(\lambda + g\varphi)\Delta t\Big]\mathrm{d}\varphi \;\propto\; -\mathrm{i}\sin(\lambda\Delta t). \tag{7.20}$$

Thus, the Yukawa transition probability strictly follows $\mathbb{P}^{\text{Yukawa}}_{L\to R} \propto \sin^2(\lambda t)$. Our QED model results reveal two key features:

(i) Initial-stage universality: Initially, the QED transition probability (for both $e = 1$ and $e = 5$) coincides perfectly with the single-boson case. Since the bosonic fields φ_k are negligible at early times, the dynamics are dominated by the mass term λ, rendering the probability independent of the boson number or coupling e.

(ii) Long-time oscillation: Subsequently, the probability exhibits stable Rabi oscillations between 0 and 1. Notably, the QED oscillation frequency is nearly double that of the Yukawa model. This doubling corresponds to the two transverse photon polarization modes represented by the bosonic components in the QED model.

8 Conclusion

In summary, this work presents a rigorous framework for formulating and computing real-time quantum field dynamics. By establishing a precise correspondence between quantum fields and classical stochastic processes, we have shown that the complex phase interference inherent in the Feynman path integral can be exactly mapped onto the probabilistic evolution of Wiener and Poisson processes.

Our applications to the Yukawa and QED models validate this formalism, revealing non-trivial dynamical features such as feedback-driven mass oscillations that elucidate non-perturbative dynamics. Crucially, this stochastic formulation is applicable to local quantum

field theories, laying a robust foundation for tackling complex systems, particularly non-Abelian gauge theories like QCD. Future work will focus on extending this framework to explore real-time non-perturbative effects, such as confinement and chiral symmetry breaking, within the context of strong interactions.

Acknowledgement: The author gratefully acknowledges Professor James Glimm from Stony Brook University. His introduction to the Feynman-Kac formalism motivated this research, and his insightful discussions on fermions and strong coupling problems were instrumental to the success of this paper.

9 Appendix

In this appendix we re-derive the classical analytic expression for the transition amplitude of a one-dimensional harmonic oscillator under a constant external source. Let the state function of the oscillator be $\varphi(t)$ with the Lagrangian action

$$\mathcal{L} = S[\varphi(t)] = \int \mathrm{d}t \Big[\frac{1}{2}\dot{\varphi}^2 - \frac{1}{2}\omega^2\varphi^2 + J_0\varphi\Big]. \tag{9.1}$$

We wish to compute the transition amplitude for the particle to go from an initial state $\varphi(0) = a$ to a final state $\varphi(T) = b$ via all possible paths:

$$K(b, T; a, 0) = \int_{\varphi(0)=a}^{\varphi(T)=b} \mathcal{D}\varphi \; e^{\mathrm{i}S[\varphi]}. \tag{9.2}$$

Following Feynman's approach [5], we decompose $\varphi(t)$ into a classical solution $x_c(t)$ and a fluctuation part $y(t)$:

$$\varphi(t) = x_c(t) + y(t), \tag{9.3}$$

where the classical solution $x_c(t)$ satisfies the driven equation of motion

$$\ddot{x}_c + \omega^2 x_c = J_0, \tag{9.4}$$

together with the boundary conditions $x_c(0) = a$, $x_c(T) = b$. The fluctuation $y(t)$ obeys zero boundary conditions, $y(0) = y(T) = 0$. The action then splits into three pieces:

$$S[\varphi(t)] = S[x_c(t)] + S[y(t)] + S_{xy}. \tag{9.5}$$

The cross term S_{xy} vanishes due to the zero boundary conditions of y and the fact that x_c satisfies (9.4):

$$S_{xy} = \int_0^T \big(\dot{x}_c\dot{y} - \omega^2 x_c y + J_0 y\big)\mathrm{d}t = \Big[\dot{x}_c(t)y(t)\Big]\Big|_0^T + \int_0^T \big(-\ddot{x}_c - \omega^2 x_c + J_0\big)y\,\mathrm{d}t = 0.$$

The second term is the action of the homogeneous harmonic oscillator (containing no source term):

$$S[y(t)] = \int \mathrm{d}t\Big[\frac{1}{2}\dot{y}^2 - \frac{1}{2}\omega^2 y^2\Big].$$

The first term is the action of the classical solution:

$$S[x_c(t)] = \int \mathrm{d}t\Big[\frac{1}{2}\dot{x}_c^2 - \frac{1}{2}\omega^2 x_c^2 + J_0 x_c\Big],$$

which is a constant with respect to the path integral and can be taken outside. Hence,

$$K(b,T;a,0) = e^{\mathrm{i}S[x_c(t)]}\int_{y(0)=0}^{y(T)=0}\mathcal{D}y\; e^{\mathrm{i}S[y]}. \tag{9.6}$$

The remaining path integral is the propagator of a free harmonic oscillator from 0 to 0, whose analytic form is known [5]:

$$K(b,T;a,0) = \sqrt{\frac{\omega}{2\pi\mathrm{i}\,\sin(\omega T)}}\; e^{\mathrm{i}S[x_c(t)]}. \tag{9.7}$$

Thus, the problem reduces to computing the classical action $S[x_c(t)]$.

According to the equation of motion (9.4), the classical solution can be written as

$$x_c(t) = A\cos(\omega t) + B\sin(\omega t) + \frac{J_0}{\omega^2}. \tag{9.8}$$

Using the boundary conditions $x_c(0) = a$ and $x_c(T) = b$, we obtain

$$\begin{aligned} A &= a - j, \\ B &= \frac{1}{\sin\theta}\Big[(b-j) - (a-j)\cos\theta\Big], \end{aligned} \tag{9.9}$$

where, for convenience, we have introduced the abbreviations

$$j = \frac{J_0}{\omega^2}, \qquad \theta = \omega T.$$

We now proceed to evaluate the action. For a solution $x_c(t)$ satisfying the equation of motion,

$$\frac{\mathrm{d}}{\mathrm{d}t}(\dot{x}_c x_c) = \dot{x}_c^2 + x_c\ddot{x}_c = \dot{x}_c^2 - \omega^2 x_c^2 + J_0 x_c.$$

Therefore,

$$S[x_c(t)] = \int_0^T \Big[\frac{1}{2}\big(\dot{x}_c^2 - \omega^2 x_c^2\big) + J_0 x_c\Big]\,\mathrm{d}t = \frac{1}{2}\int_0^T \frac{\mathrm{d}}{\mathrm{d}t}(\dot{x}_c x_c)\,\mathrm{d}t + \frac{1}{2}J_0\int_0^T x_c(t)\,\mathrm{d}t.$$

The first term gives

$$\begin{aligned}
\frac{1}{2}\int_0^T \frac{\mathrm{d}}{\mathrm{d}t}(\dot{x}_c x_c)\,\mathrm{d}t &= \frac{1}{2}\Big[\dot{x}_c(T)b - \dot{x}_c(0)a\Big] \\
&= \frac{1}{2}\Big[-A\omega\sin\theta + B\omega\cos\theta\Big]b - \frac{1}{2}B\omega a \\
&= -\frac{(a-j)}{2}\omega b\sin\theta + \frac{(b-j)-(a-j)\cos\theta}{2\sin\theta}\,\omega\,(b\cos\theta - a) \\
&= \frac{\omega}{2\sin\theta}\Big[-ab\sin^2\theta + (b\cos\theta - a)(b - a\cos\theta)\Big] \\
&\qquad + \frac{j\omega}{2\sin\theta}\Big[b\sin^2\theta - (1-\cos\theta)(b\cos\theta - a)\Big] \\
&= \frac{\omega}{2\sin\theta}\Big[(a^2+b^2)\cos\theta - 2ab\Big] + \frac{j\omega}{2\sin\theta}(a+b)(1-\cos\theta).
\end{aligned}$$

The second term is

$$\begin{aligned}
\frac{J_0}{2}\int_0^T x_c(t)\,\mathrm{d}t &= \frac{J_0}{2}\int_0^T \Big[A\cos(\omega t) + B\sin(\omega t) + j\Big]\,\mathrm{d}t \\
&= \frac{J_0}{2\omega}\Big[A\sin\theta + B(1-\cos\theta) + j\theta\Big] \\
&= \frac{J_0}{2\omega}\Big[(a-j)\sin\theta + \frac{1}{\sin\theta}\big(b - j - (a-j)\cos\theta\big)(1-\cos\theta) + j\theta\Big] \\
&= \frac{J_0}{2\omega\sin\theta}\Big[a\sin^2\theta + (b - a\cos\theta)(1-\cos\theta)\Big] \\
&\qquad + \frac{J_0 j}{2\omega\sin\theta}\Big[-\sin^2\theta - (1-\cos\theta)^2 + \theta\sin\theta\Big] \\
&= \frac{J_0}{2\omega\sin\theta}(a+b)(1-\cos\theta) + \frac{J_0 j}{2\omega\sin\theta}\Big[\theta\sin\theta - 2(1-\cos\theta)\Big].
\end{aligned}$$

Adding the two terms and substituting $j = J_0/\omega^2$ and $\theta = \omega T$ yields

$$\begin{aligned} S[x_c(t)] &= \frac{\omega}{2\sin(\omega T)}\Big[(a^2+b^2)\cos(\omega T) - 2ab\Big] \\ &\quad + \frac{J_0}{\omega\sin(\omega T)}(a+b)\big(1-\cos(\omega T)\big) \\ &\quad + \frac{J_0^2}{2\omega^3\sin(\omega T)}\Big[\omega T\sin(\omega T) - 2\big(1-\cos(\omega T)\big)\Big]. \end{aligned} \tag{9.10}$$

Inserting $S[x_c(t)]$ into (9.7) gives the complete analytic expression for $K(b,T;a,0)$. In particular, for $a = 0$ we obtain

$$\begin{aligned} K(b,T;0,0) &= \sqrt{\frac{\omega}{2\pi\mathrm{i}\,\sin(\omega T)}}\cdot\exp\Big\{\mathrm{i}\,\frac{b^2\omega}{2}\frac{\cos(\omega T)}{\sin(\omega T)} \\ &\quad + \mathrm{i}\,\frac{bJ_0}{\omega}\frac{1-\cos(\omega T)}{\sin(\omega T)} + \mathrm{i}\frac{J_0^2}{2\omega^3}\Big(\omega T - 2\frac{1-\cos(\omega T)}{\sin(\omega T)}\Big)\Big\}. \end{aligned} \tag{9.11}$$

References

[1] M. E. Peskin and D. V. Schroeder, *An Introduction to Quantum Field Theory*, Westview Press, Boulder, 1995, Section 4.2.

[2] K. G. Wilson, Confinement of quarks, *Phys. Rev. D* **10**, 2445–2459 (1974).

[3] M. Troyer and U.-J. Wiese, Computational complexity and fundamental limitations to fermionic quantum Monte Carlo simulations, *Phys. Rev. Lett.* **94**, 170201 (2005).

[4] D. B. Kaplan, A method for simulating chiral fermions on the lattice, *Phys. Lett. B* **288**, 342–347 (1992).

[5] R. P. Feynman and A. R. Hibbs, *Quantum Mechanics and Path Integrals*, McGraw-Hill, New York, 1965, pp. 170–177.

[6] J. Glimm and A. Jaffe, *Quantum Physics: A Functional Integral Point of View*, 2nd ed., Springer-Verlag, New York, 1987.

[7] G. N. Ord, Stochastic quantization and path integrals, *J. Phys. A: Math. Gen.* **16**, 1869–1885 (1983).

[8] T. Jacobson and L. S. Schulman, Quantum stochastic processes: A path integral approach, *J. Phys. A: Math. Gen.* **17**, 375–388 (1984).

[9] G. Strang, Accurate partial difference methods, II nonlinear problems, *Numer. Math.* **13**, 37–46 (1964).

[10] C. J. Burden, Fermion mass generation in the (1+1)-dimensional Yukawa model, *Nucl. Phys. B* **387**, 419–446 (1992).

[11] S. A. Chin, Yukawa model in 1+1 dimensions, *Phys. Rev. D* **42**, 699–706 (1990).